



**HAL**  
open science

## **5-oxoETE triggers nociception in constipation-predominant irritable bowel syndrome through MAS-related G protein-coupled receptor D**

Tereza Bautzova, James Hockley, Teresa Pérez-Berezo, Julien Pujo, Michael Tranter, Cléo Desormeaux, Maria Raffaella Barbaro, Lilian Basso, Pauline Le Faouder, Corinne Rolland, et al.

### ► To cite this version:

Tereza Bautzova, James Hockley, Teresa Pérez-Berezo, Julien Pujo, Michael Tranter, et al.. 5-oxoETE triggers nociception in constipation-predominant irritable bowel syndrome through MAS-related G protein-coupled receptor D. *Science Signaling*, 2018, 11 (561), pp.eaal2171. 10.1126/scisignal.aal2171 . hal-02092494

**HAL Id: hal-02092494**

**<https://hal.science/hal-02092494>**

Submitted on 29 Apr 2019

**HAL** is a multi-disciplinary open access archive for the deposit and dissemination of scientific research documents, whether they are published or not. The documents may come from teaching and research institutions in France or abroad, or from public or private research centers.

L'archive ouverte pluridisciplinaire **HAL**, est destinée au dépôt et à la diffusion de documents scientifiques de niveau recherche, publiés ou non, émanant des établissements d'enseignement et de recherche français ou étrangers, des laboratoires publics ou privés.

1 **Title: 5-oxoETE triggers nociception in constipation predominant irritable bowel**  
2 **syndrome through MAS-related G protein coupled receptor D**

3  
4 **Authors:** Tereza Bautzova<sup>1†</sup>, James RF Hockley<sup>2,3†</sup>, Teresa Perez-Berezo<sup>1†</sup>, Julien Pujol<sup>1</sup>,  
5 Michael M Tranter<sup>3</sup>, Cleo Desormeaux<sup>1</sup>, Maria Raffaella Barbaro<sup>5</sup>, Lilian Basso<sup>1#</sup>, Pauline Le  
6 Faouder<sup>4</sup>, Corinne Rolland<sup>1</sup>, Pascale Malapert<sup>6</sup>, Aziz Moqrich<sup>6</sup>, Helene Eutamene<sup>7</sup>, Alexandre  
7 Denadai-Souza<sup>1</sup>, Nathalie Vergnolle<sup>1</sup>, Ewan St John Smith<sup>2</sup>, David I Hughes<sup>8</sup>, Giovanni  
8 Barbara<sup>5</sup>, Gilles Dietrich<sup>1</sup>, David Bulmer<sup>2,3</sup>, Nicolas Cenac<sup>1\*</sup>

9 **Affiliations:**

10 <sup>1</sup> INSERM, UMR1220, IRSD, Université de Toulouse, INRA, ENVT, UPS, Toulouse, France

11 <sup>2</sup> Department of Pharmacology, University of Cambridge, Tennis Court Road, Cambridge  
12 CB1 2PD, UK

13 <sup>3</sup> National Centre for Bowel Research and Surgical Innovation, Blizard Institute, Barts and  
14 the London School of Medicine and Dentistry, Queen Mary University of London, London E1  
15 2AJ, UK

16 <sup>4</sup> INSERM UMR1048, Lipidomic Core Facility, Metatoul Platform, Université de Toulouse,  
17 Toulouse, France

18 <sup>5</sup> Department of Medical and Surgical Sciences, University of Bologna, Bologna, Italy

19 <sup>6</sup> Aix-Marseille-Université, CNRS, Institut de Biologie du Développement de Marseille,  
20 UMR 7288, Marseille, France.

21 <sup>7</sup> Neuro-Gastroenterology and Nutrition Team, UMR 1331, INRA Toxalim, INP-EI-Purpan,  
22 Université de Toulouse, Toulouse, France

23 <sup>8</sup> Institute of Neuroscience and Psychology, University of Glasgow, Glasgow, United  
24 Kingdom

25  
26 † Joint as first author

27 # Current address: Snyder Institute for Chronic Diseases, Cumming School of Medicine,  
28 University of Calgary, 3330 Hospital Drive N.W., Calgary, Alberta, Canada, T2N 4N1

29  
30 **\* Corresponding author:**

31 Nicolas Cenac

32 INSERM IRSD U1220

33 CHU Purpan

34 Place du docteur Baylac ; CS 60039

35 31024 Toulouse cedex 3 ; France

36 +33531 547 917

37 [nicolas.cenac@inserm.fr](mailto:nicolas.cenac@inserm.fr)

38  
39  
40 **One Sentence Summary:** The bioactive lipid 5-oxoETE is specifically increased in  
41 constipation predominant irritable bowel syndrome and mediates nociception through a novel  
42 MAS-related G protein coupled receptor D (Mrgprd) pathway.

43 **Abstract**

44 Irritable bowel syndrome (IBS) is a common gastrointestinal disorder characterized by  
45 chronic abdominal pain concurrent with altered bowel habit. Polyunsaturated fatty acid (PUFA)  
46 metabolites such as prostaglandin E2 (PGE<sub>2</sub>) are elevated in IBS and implicated in visceral  
47 hypersensitivity. The aim of this study was to quantify PUFA metabolites in IBS patients and  
48 evaluate their role in pain. Quantification of PUFA metabolites by mass spectrometry in colonic  
49 biopsies showed an increase in 5-oxo-eicosatetraenoic acid (5-oxoETE) only in biopsies taken  
50 from IBS with predominant constipation (IBS-C) patients. Local 5-oxoETE administration  
51 induced somatic and visceral hypersensitivity with no tissue inflammation. 5-oxoETE directly  
52 acts on both human and mouse sensory neurons as shown by lumbar splanchnic nerve  
53 recordings and Ca<sup>2+</sup>-imaging of dorsal root ganglia (DRG) neurons. 5-oxoETE selectively  
54 stimulated isolectin B4 (IB4)-positive DRG neurons through a PLC and pertussis toxin-  
55 dependent mechanism, suggesting a G-protein coupled receptor-mediated effect. The MAS-  
56 related G protein coupled receptor D (Mrgprd) was found in mouse colonic DRG afferents and  
57 was identified as the target receptor for 5-oxoETE. In conclusion, 5-oxoETE, a potential  
58 biomarker of IBS-C, activates Mrgprd in nociceptors and induces somatic and visceral  
59 hyperalgesia without inflammation. Thus, 5-oxoETE may play a pivotal role in abdominal pain  
60 associated with IBS-C.

61

## 62 **Introduction**

63 IBS is a functional bowel disorder in which recurrent abdominal pain is associated with  
64 a change in bowel habit, typically constipation (IBS-C), diarrhea (IBS-D), or a mixed  
65 (constipation and diarrhea) bowel habit (IBS-M) (1). IBS is a common disorder in Western  
66 populations affecting around 11% of the global population (2), with a higher prevalence in  
67 women than men (1). Although the aetiology of IBS remains unclear, low-grade inflammation  
68 has been widely described in this disorder, with several fundamental studies implicating pro-  
69 inflammatory molecules in the pathophysiology of IBS symptoms (3). We have previously  
70 shown that the levels of several PUFA metabolites, also defined as bioactive lipids, are  
71 significantly altered in biopsy samples from IBS patients compared to controls (4). This is in  
72 agreement with previous studies focused on the prostanoid subtype of PUFA metabolites (5-7).

73 The functional relationship between PUFAs and pain has been the subject of many  
74 studies (8). Both basic and clinical studies have revealed that a dietary intake of n-3 series  
75 PUFAs results in a reduction in pain associated with rheumatoid arthritis (9, 10), dysmenorrhea  
76 (11), inflammatory bowel disease (12), and neuropathy (13), while n-6 series PUFAs are high  
77 in patients with chronic pain including IBS patients (4, 14, 15). N-3 PUFA metabolites such as  
78 resolvins (Rv) are analgesic in multiple pain models, an effect attributed to inhibition of certain  
79 transient receptor potential (TRP) channels (16). For example, RvE1 has been shown to  
80 specifically inhibit TRPV1 signaling (17), while RvD1 attenuates the function of TRPA1 and  
81 TRPV4 (18) and RvD2 inhibits TRPV1 and TRPA1 activity (19). These effects have been  
82 observed with other types of n-3 PUFAs such as maresin 1 (Mar1), which also has inhibitory  
83 effects on TRPV1 channel function (20) and reduces pain. The quantification of Rvs in knee  
84 synovia of patients suffering from inflammatory arthritis suggests that synthesis of specialized  
85 pro-resolving mediators (SPM) at the site of inflammation may be a mechanism of endogenous  
86 pain relief in humans. In contrast, n-6 PUFA metabolites have been shown to be pro-nociceptive

87 by stimulating nerve fibers via the activation of immune cells (21, 22). Nonetheless, several n-  
88 6 PUFA metabolites such as thromboxane A<sub>2</sub> (TXA<sub>2</sub>), PGE<sub>2</sub>, leukotriene B<sub>4</sub> (LtB<sub>4</sub>) and PGD<sub>2</sub>,  
89 can directly stimulate sensory nerve fibers (23-26). Although, some n-6 PUFA metabolites,  
90 such as lipoxins, can inhibit pain (27). Consistent with the role of TRP channels in the  
91 transduction of noxious stimuli, we have previously shown a robust correlation between PUFA  
92 metabolites and TRP channel activation, particularly for the TRPV4 agonist 5,6-  
93 epoxyeicosatrienoic acid (5,6-EET) and pain intensity in IBS-D patients (4). Interestingly,  
94 PUFA metabolites from colonic biopsies of IBS-C patients induced Ca<sup>2+</sup> influx in sensory  
95 neurons independently of TRPV4, suggesting that the PUFA metabolites produced in IBS-C  
96 and IBS-D are distinct (4). Thus, the aim of this study was to identify algogenic PUFA  
97 metabolites specifically produced in IBS-C patients and decipher the mechanism by which they  
98 may activate sensory nerves. Herein, we show that 5-oxoETE, an n-6 PUFA subtype selectively  
99 increased in colonic tissues from IBS-C patients, induces hypersensitivity through Mrgprd  
100 activation.

101

102

103

104 **Results**

105 **5-oxoETE is increased in colonic biopsies from IBS-C patients**

106 PUFA metabolites were quantified in colonic biopsies from IBS patients and healthy controls  
107 (HC) using liquid chromatography/tandem mass spectrometry (LC-MS/MS). Hierarchical  
108 clustering of PUFA metabolite amounts quantified in biopsies (pg/mg of protein) was used to  
109 reveal the main differences between HC, IBS-M, IBS-C and IBS-D patients (Fig.1A). PUFA  
110 metabolites formed 5 different clusters. The first cluster contained products of arachidonic acid  
111 metabolism (PGE<sub>2</sub>, TXB<sub>2</sub>, 5,6-EET and 14,15-EET), eicosapentaenoic acid metabolism (18-  
112 HEPE, LtB5 and PGE<sub>3</sub>) and PDx. This first cluster of metabolites was higher in biopsies from  
113 IBS-D patients (Fig.1A). Of note, TxB<sub>2</sub>, PGE<sub>2</sub> and 5,6-EET were only increased in biopsies of  
114 IBS-D patients (Fig. S1). By contrast, TxB<sub>2</sub> was decreased in biopsies from IBS-C patients (Fig.  
115 S1). The second cluster discriminated only 5-oxoETE, which was significantly elevated in  
116 biopsies from IBS-C patients (Fig.1A and 1B). The concentration of 7-MaR1 and 15dPGJ<sub>2</sub>,  
117 delineated a third cluster, which although presenting a trend towards increasing levels, did not  
118 reach statistical significance in biopsies from any group of IBS patients (Fig. S2). The fourth  
119 cluster, grouping the majority of lipoxygenase-derived metabolites, was decreased in biopsies  
120 from all subtypes of IBS patients (Fig.1A). 15-, 5-, 12-HETE and 14-, 17-HDoHE were  
121 significantly decreased in all IBS patients (Fig. S2). In addition, 12-HETE was significantly  
122 decreased in biopsies from IBS-C patients (Fig. S1). The metabolites included in the fifth cluster  
123 were reduced only in biopsies from IBS-C and IBS-D (Fig.1A). RvD1 and RvD2 were not  
124 detectable in any colonic biopsies.

125 Thus, amongst all PUFA metabolites quantified in colonic biopsies from IBS patients,  
126 5-oxoETE was the only one to be significantly upregulated in IBS-C patients compared to the  
127 other IBS subtypes (Fig.1B) and thus warranted further investigation.

128

129 **Local administration of 5-oxoETE induces somatic and visceral hyperalgesia without**  
130 **inflammation**

131 As PUFA metabolites can stimulate the immune system and/or directly stimulate nerves,  
132 we first assessed the effect of 5-oxoETE on pain and inflammation processes *in vivo*. In a first  
133 set of experiments, 5-oxoETE was subcutaneously injected into the paw of mice and the paw-  
134 withdrawal threshold to mechanical stimuli was estimated using calibrated von Frey filaments.  
135 The time course of mechanical hypersensitivity of the mice receiving 5-oxoETE was compared  
136 with that of mice injected with vehicle (HBSS). Basal mechanical sensitivity, measured in the  
137 paw before injection, was identical in both groups of mice (Fig.2A). Injection of 5-oxoETE into  
138 hind paws resulted in a decrease of the paw-withdrawal threshold (Fig.2A) and was observed  
139 from 15 min up to 2 hours after 5-oxoETE injection, with a peak reduction at 30 min. The  
140 mechanical pain threshold was decreased in a dose-dependent manner 30 min after 5-oxoETE  
141 administration with an EC<sub>50</sub> of 0.6 μM (Fig.2B). In addition, paw edema formation and  
142 histological analysis were investigated to verify whether injection of 5-oxoETE induced an  
143 inflammatory process or not. Injection of 5-oxoETE into the hind paw did not induce paw  
144 edema (Fig. S3). Moreover, histological analysis of paw tissue did not reveal any sign of  
145 inflammation. Likewise, neither tissue disruption nor cellular infiltration was observed even 6  
146 hours after injection of 100 μM of 5-oxoETE (Fig.2C). Thus, at the somatic level, 5-oxoETE  
147 increased paw sensitivity to mechanical stimulation without inducing quantifiable  
148 inflammatory reaction.

149 Intracolonic administration of 5-oxoETE resulted in an increased intensity of abdominal  
150 contractions in response to colorectal distension (Fig.2D). Moreover, the increased intensity of  
151 abdominal contractions was observed in response to both innocuous (allodynia) and noxious  
152 (hyperalgesia) stimuli 30 min after 5-oxoETE treatment (Fig.2D). Intracolonic treatment with  
153 vehicle (40% ethanol) did not alter abdominal contraction response (Fig.2D). As observed

154 following subcutaneous hind paw injection, intracolonic administration of 5-oxoETE did not  
155 induce inflammation of the colon. Colonic inflammation was assessed by macroscopic scoring  
156 and myeloperoxidase activity, which were not increased by 5-oxoETE administration when  
157 compared to vehicle (Fig. S3). Moreover, histological analysis did not reveal intestinal wall  
158 thickening, leukocyte infiltration into the *lamina propria*, presence of ulceration or goblet cell  
159 depletion (Fig.2E).

160 Thus, *in vivo* local administration of 5-oxoETE induces visceral hyperalgesia in the  
161 absence of inflammation, thus suggesting a direct effect on nociceptors.

162

### 163 **5-oxoETE stimulates visceral and somatic nociceptors: translation to human DRG**

164 To confirm a direct effect of 5-oxoETE on sensory nerves, we examined its effects upon  
165 nerve discharge in mouse colonic nociceptors. Application of 100  $\mu\text{M}$  of 5-oxoETE induced an  
166 axonal discharge in 38% of lumbar splanchnic (colonic) nerve fibers assessed (Fig.3). In a  
167 second set of experiments, we determined the effect of 5-oxoETE on  $\text{Ca}^{2+}$  mobilization in  
168 primary cultures of neurons from mouse DRG. In preliminary experiments performed with a  
169 working solution containing  $\text{Ca}^{2+}$  and  $\text{Mg}^{2+}$ , we observed a transient increase in  $[\text{Ca}^{2+}]_i$  (data  
170 not shown). To determine if this transient increase was the consequence of intracellular  $\text{Ca}^{2+}$   
171 release or influx of external  $\text{Ca}^{2+}$ , experiments were performed without  $\text{Ca}^{2+}$  and  $\text{Mg}^{2+}$  in the  
172 extracellular solution. Even without  $\text{Ca}^{2+}$  in the extracellular compartment, 5-oxoETE evoked  
173 a transient increase in  $[\text{Ca}^{2+}]_i$  that was maximal after 10–20 seconds and declined to baseline  
174 afterwards (Fig.4A). The mobilization of intracellular  $\text{Ca}^{2+}$  by 5-oxoETE treatment was  
175 concentration-dependent (Fig.4B). Similarly, 5-oxoETE also induced an increase in  $[\text{Ca}^{2+}]_i$  and  
176 the percentage of responding neurons in a concentration-dependent manner in human primary  
177 sensory neurons (Fig.4C).



178 Thus, our data indicate that 5-oxoETE directly activates colonic DRG neurons from  
179 mice, as well as human sensory neurons, inducing an increase in  $[Ca^{2+}]_i$  (Fig.4) and nociceptor  
180 firing (Fig.3).

181 As 5-oxoETE induces somatic pain without inflammation *in vivo*, we hypothesised that  
182 5-oxoETE predominantly activates IB4<sup>+</sup> sensory neurons, which do not release neuropeptides  
183 involved in neurogenic inflammation. To assess our hypothesis, mouse sensory neurons were  
184 labelled with isolectin B4 and treated with 10  $\mu$ M 5-oxoETE without  $Ca^{2+}$  in the extracellular  
185 medium. 5-oxoETE induced an increase in  $[Ca^{2+}]_i$  in more than 50% of IB4-positive neurons,  
186 but not in IB4-negative neurons (Fig.4D). To decipher the intracellular pathway responsible for  
187 the intracellular  $Ca^{2+}$  mobilization by 5-oxoETE, sensory neurons were pretreated with  
188 pertussis toxin (PTX, a  $G_i$ , G protein inhibitor) or the PLC inhibitor U73122. In neurons  
189 pretreated with the pertussis toxin (PTX; 250 ng/ml), the increase in  $[Ca^{2+}]_i$  induced by 5-  
190 oxoETE was significantly decreased (Fig.4E). Pre-treatment of sensory neurons with U73122  
191 (10 $\mu$ M) also inhibited the increase in  $[Ca^{2+}]_i$  induced by 5-oxoETE (Fig.4E).

192 Thus, 5-oxoETE directly stimulates IB4-positive sensory neurons via a  $G\alpha_{i/o}/G\alpha_q$ -  
193 coupled, G-protein-coupled receptor.

194

### 195 **5-oxoETE activates sensory neurons and induces visceral hypersensitivity via Mrgprd**

196 Due to 5-oxoETE specifically activating IB4<sup>+</sup> sensory neurons via  $G\alpha_i$ -protein-  
197 mediated signalling pathways, we focused our attention on the MAS-related G protein receptor  
198 D (Mrgprd), which is  $G\alpha_{i/o}/G\alpha_q$  coupled. The expression and function of Mrgprd in polymodal  
199 nociceptors innervating the skin is well established (28), however for visceral tissues this  
200 remains less clear. In order to comprehensively assess this, we retrogradely labelled sensory  
201 afferents from the colon using microinjection of Fast Blue (FB) in wild-type mice and  
202 *Mrgprd*<sup>EGFP</sup>-tagged mice. Single-cell qRT-PCR was performed on FB-expressing cells from

203 the dorsal root ganglia from wild-type mice. *Mrgprd* mRNA was detected at some level in 40%  
204 (18/45) of FB-labelled sensory neurons projecting to the colon via the splanchnic nerve  
205 originating from thoracolumbar (T10-L1) DRG (Fig.5A). *Trpv1* mRNA was observed in 82%  
206 (37/45) of cells, with 41% (15/37) of *Trpv1*-positive neurons also expressing *Mrgprd* mRNA  
207 (Fig.5A). Immunohistochemistry was performed on the T13 DRG from the *Mrgprd*<sup>EGFP</sup>-tagged  
208 mice to determine the incidence of GFP-expression and the peptidergic marker calcitonin gene  
209 related peptide (CGRP) in FB-labelled cells, revealing two distinct non-overlapping  
210 populations (Fig.5B). In agreement with previous studies, those sensory neurons labelled from  
211 the colon with the retrograde tracer Fast-Blue were predominantly CGRP-positive (~70%). By  
212 contrast, GFP immunoreactivity was observed in a restricted subset of colonic sensory neurons,  
213 accounting for only 7% of FB-labelled cells (Fig. 5B and Table 2). Of the 274 FB+ cells  
214 assessed, only cell one co-expressed both *Mrgprd* and CGRP. Those neurons projecting to the  
215 viscera represent ~10% of the total population of T10-L1 DRG neurons. Thus, only a very small  
216 population (between less than 1% and 4%) of T10-L1 DRG neurons are likely to be both colon  
217 projecting and *Mrgprd*-positive.

218 In experiments using an antibody against *Mrgprd*, we observed, infrequent yet  
219 reproducible, co-localisation of *Mrgprd* with PGP9.5 in the colon of 6 wild-type mice out of 10  
220 assessed (Fig.S4). Importantly, *Mrgprd* immunoreactivity was not observed in the colon of  
221 *Mrgprd*-deficient mice (Fig.S4). The expression of *Mrgprd* was also assessed in human sensory  
222 neurons. As shown in Fig.5C, *Mrgprd* immunoreactivity was present in 22% of human T11  
223 DRG neurons, which also co-expressed the pan-neuronal marker PGP9.5. In a culture of human  
224 sensory neurons, 20% of PGP9.5-positive neurons possessed *Mrgprd* immunoreactivity  
225 (Fig.5D).

226 To demonstrate the role of *Mrgprd* in 5-oxoETE-induced neuronal firing, its expression  
227 was silenced by transducing primary cultures of mouse sensory DRG neurons with a

228 recombinant lentivirus expressing a shRNA directed against *Mrgprd* and the gene reporter red  
229 fluorescent protein (RFP). As a control, neurons were transduced with a lentivirus expressing a  
230 scrambled shRNA. As expected, the percentage of neurons responding to 5-oxoETE was  
231 significantly reduced in sensory neurons expressing shRNA against *Mrgprd* compared to those  
232 neurons expressing the scrambled shRNA (Fig.6A). Accordingly, application of 5-oxoETE on  
233 sensory neurons from *Mrgprd*-deficient mice had no greater effect than HBSS alone (Fig.6B).  
234 In contrast, treatment of *Mrgprd*-deficient sensory neurons with a mix of GPCR agonists  
235 (bradykinin, serotonin and histamine, 10  $\mu$ M each), used as a positive control, induced an  
236 increase in  $[Ca^{2+}]_i$  (Fig.6B). Reciprocally, 5-oxoETE induced a concentration-dependent  
237 increase in  $[Ca^{2+}]_i$  only in *Mrgprd*-transfected CHO cells (Fig.6C). In a last set of experiments,  
238 the sensitivity to colorectal distension was assessed in *Mrgprd*-deficient mice 30 min after  
239 intracolonic administration of 5-oxoETE (10  $\mu$ M). In contrasting to wild-type mice, 5-oxoETE  
240 did not induce hypersensitivity in response to colorectal distension in *Mrgprd*-deficient mice  
241 (Fig.6D).

242

243 **Discussion**

244 Our results show that: 1) Concentrations of the PUFA metabolite 5-oxoETE are  
245 significantly increased in biopsies from patients with IBS-C compared to other IBS subtypes  
246 and healthy controls; 2) 5-oxoETE induces somatic, as well as visceral hyperalgesia, without  
247 promoting inflammation; 3) 5-oxoETE activates both mouse and human sensory neurons; 4) In  
248 mouse, 5-oxoETE signals through Mrgprd. Taken together, these data clearly highlight a role  
249 for 5-oxoETE and Mrgprd-expressing IB4-positive sensory neurons in visceral hypersensitivity  
250 in IBS-C patients.

251 Eicosanoids and docosanoids are the most important lipids implicated in inflammatory  
252 processes; they derive from the oxidation of twenty and twenty-two carbon PUFA, respectively  
253 (29). Several PUFA metabolites increased in the intestinal mucosa from patients with  
254 inflammatory bowel diseases such as TXA<sub>2</sub>, PGE<sub>2</sub>, LTB<sub>4</sub> or PGD<sub>2</sub> induce visceral afferent fiber  
255 activation (23-26). Here, we show that PGE<sub>2</sub>, 5,6-EET and TXB<sub>2</sub> are significantly increased in  
256 the intestinal mucosa of IBS-D patients while no alteration of PUFA metabolism was observed  
257 in IBS-M. Interestingly, if lipid extracts from controls and all IBS patients are compared, a  
258 significant decrease in 14-HDoHE and 17-HDoHE which are precursors of specialized pro-  
259 resolving mediators (SPM) (30), is observed. As SPM possess an analgesic effect (31), the pain  
260 associated with IBS could be also the consequence of a decrease in SPM leading to sensory  
261 neuron activation. A complete characterization of the different SPM produced by EPA, DHA  
262 or DPA metabolism will be of interest for the characterization of bioactive lipids potentially  
263 linked with pain in IBS patients.

264 We show that the concentration of 5-oxoETE only increases in colonic biopsies of IBS-  
265 C patients highlighting its potential relevance as a new marker of the disease. 5-oxoETE, which  
266 derives from arachidonic acid (AA) metabolism, is produced by a variety of inflammatory cells.  
267 Additionally, it can also be synthesized from 5-HETE by stromal cells, possibly by transcellular

268 biosynthesis (32). 5-oxoETE is formed by the oxidation of 5-HETE by 5-hydroxyeicosanoid  
269 dehydrogenase (5-HEDH) (33), a microsomal enzyme that is highly selective for 5S-HETE and  
270 requires NADP<sup>+</sup> as a cofactor (34). 5-HEDH is found in neutrophils as well as in a variety of  
271 other inflammatory and stromal cells, including monocytes (35), dendritic cells (36) and  
272 intestinal epithelial cells (37). 5-oxoETE has been widely shown to be a potent chemoattractant  
273 for human and rat eosinophils and to indirectly promote the survival of these cells (38).  
274 Nevertheless, no cellular infiltration was observed either in the paw or intestinal mucosa of  
275 mice administered with 5-oxoETE. This discrepancy may be due to the rapid metabolism of 5-  
276 oxoETE *in vivo* (32) or the absence of other molecules such as interleukin-5 acting in synergy  
277 to attract inflammatory cells during inflammatory processes or allergies (39). In our  
278 experiments, the injection of 5-oxoETE alone, without cofactors, could thus explain the absence  
279 of infiltration by polymorphonuclear cells. Formation of 5-oxoETE needs NADP<sup>+</sup> (40).  
280 Accordingly, oxidative stress associated with IBS-C (41) may improve the conversion rate of  
281 NADPH into NADP<sup>+</sup> in epithelial cells, thereby resulting in the synthesis of larger amounts of  
282 5-oxoETE.

283         In a previous study, we reported that PUFA metabolites extracted from biopsies of IBS-  
284 C and IBS-D patients triggered an increase in [Ca<sup>2+</sup>]<sub>i</sub> in primary sensory neurons, while those  
285 of IBS-M had no effect (4). We further identified the PUFA metabolite 5,6-EET as a TRPV4  
286 agonist with algogenic activity, specifically associated with IBS-D sub-group (4). By contrast,  
287 no PUFA metabolite with TRP agonist activity was found to be increased in IBS-C patient  
288 biopsies (4). Since only 5-oxoETE is increased in biopsies of IBS-C patients, we hypothesized  
289 that this PUFA metabolite may be responsible for the activation of sensory neurons and  
290 hypersensitivity-associated with IBS-C. As previously reported in humans, 5-oxoETE may  
291 interact with OXE receptor. However, there is no homologous OXE receptor in rodents (40).  
292 Since the observed 5-oxoETE-induced increase in [Ca<sup>2+</sup>]<sub>i</sub> in mouse sensory neurons was

293 inhibited by both PLC inhibitor and pertussis toxin (PTX), we hypothesized that 5-oxoETE  
294 binds to  $G\alpha_{i/o}/G\alpha_q$  protein-coupled receptors. Given that 5-oxoETE acts selectively on IB4<sup>+</sup>  
295 sensory neurons, the targeted receptor should be specifically expressed on this neuronal  
296 subclass. Accordingly, we investigated the role of MAS-related G protein coupled receptor D  
297 (Mrgprd), a receptor specifically expressed on IB4<sup>+</sup> sensory neurons, which may be coupled to  
298  $G\alpha_q$  protein and to PTX-sensitive  $G\alpha_{i/o}$  proteins (42), previously reported as a key player in  
299 mechanical hypersensitivity (43-45).

300 Stimulation of Mrgprd positive neurons with  $\beta$ -alanine, the prototypical agonist of  
301 Mrgprd, increased  $[Ca^{2+}]_i$ , as observed here after 5-oxoETE treatment (46). Moreover, in a  
302 FLIPR (Fluorescent Imaging Plate Reader) assay developed for the simultaneous identification  
303 of Mrgprd agonists and antagonists, a PLC inhibitor completely blocked the FLIPR response  
304 to  $\beta$ -alanine while PTX treatment resulted in 50% reduction in  $[Ca^{2+}]$  (47). Again, similar  
305 results were obtained here by using PTX or PLC inhibitor to inhibit 5-oxoETE-induced  
306 activation of primary mouse sensory neurons. Using tissue from adult *Mrgprd*<sup>EGFP</sup> mice stained  
307 with antibodies to GFP, a previous study showed that Mrgprd is expressed in non-peptidergic  
308 neurons that innervate the epidermis, but failed to observe Mrgprd-positive fibres in any other  
309 visceral organs including both the small and large intestine (28). By contrast, numerous studies  
310 using different retrograde tracers have identified a minor population (20-26%) of IB4<sup>+</sup> sensory  
311 neurons that innervate the colon (48-50). Indeed, a recent study also identified *Mrgprd* mRNA  
312 in colonic sensory neurons by single cell RNA-sequencing (51). In order to confirm the  
313 presence of both *Mrgprd* mRNA and Mrgprd protein expression in colonic sensory neurons in  
314 the present study, we applied a similar retrograde neurotracing approach using single cell RT-  
315 qPCR and anti-GFP immunostaining in *Mrgprd*<sup>EGFP</sup> mice. We observed *Mrgprd* mRNA and  
316 Mrgprd protein expression in sensory DRG neurons projecting to the colon at similar frequency  
317 to that observed in previous studies (51), thereby not only confirming the presence of a Mrgprd-

318 positive colonic neuronal subtype, but also reinforcing *Mrgprd* as a potential target of 5-  
319 oxoETE. The activity of 5-oxoETE towards *Mrgprd* was attested to by its ability to induce an  
320 increase in  $[Ca^{2+}]_i$  in IB4-positive sensory neurons, but not in lentivirus-mediated *Mrgprd*  
321 knocked-down or *Mrgprd*-deficient mouse neurons. Conversely, while  $Ca^{2+}$  transients were  
322 triggered in CHO cells transfected with a *Mrgprd*-expression plasmid, CHO cells transfected  
323 with a control plasmid were not responsive to 5-oxoETE.

324         Activation of *Mrgprd* inhibits a fraction of the total M-current, carried primarily by the  
325 KCNQ2/3  $K^+$  channel, contributing to an increase in excitability of DRG neurons (52). Thus,  
326 *Mrgprd* activation by 5-oxoETE might promote the excitability of primary nociceptive afferents  
327 by KCNQ inhibition. Several groups have demonstrated that retigabine, a KCNQ2–5 opener,  
328 is effective in reducing neuropathic (53) and inflammatory pain (54). At the visceral level,  
329 retigabine reduces capsaicin-induced visceral pain and can inhibit noxious chemosensitivity in  
330 human tissue indicating that KCNQ channels play an inhibitory role in the transmission of  
331 visceral nociception (55, 56). Given that human sensory DRG neurons express *Mrgprd* and are  
332 activated by 5-oxoETE, we may assume that 5-oxoETE modulates KCNQ channels via *Mrgprd*  
333 activation leading to neuronal activation contributing to pain symptoms associated with IBS-C.  
334 Nevertheless, as OXER1 is expressed in human tissue, we cannot exclude an activation of this  
335 receptor by 5-oxoETE in human tissue. Taken together, our results strengthen previous findings  
336 from our laboratory showing a pivotal role of PUFA metabolites in visceral pain associated  
337 with IBS (4). Specifically, our study identifies 5-oxoETE with pro-nociceptive activity, as a  
338 hallmark of IBS-C subtype.

339 **Materials and methods**

340 **Chemicals**

341 6-keto-prostaglandin F1 $\alpha$  (6kPGF $_{1\alpha}$ ), thromboxane B2 (TXB $_2$ ), prostaglandin E2 (PGE $_2$ ),  
342 prostaglandin A1 (PGA $_1$ ), 8-iso prostaglandin A2 (8-iso PGA $_2$ ), prostaglandin E3 (PGE $_3$ ), 15-  
343 deoxy- $\Delta^{12,14}$ -prostaglandin J2 (15d-PGJ $_2$ ), lipoxin A4 (LxA4), lipoxin B4 (LxB4), lipoxin A4  
344 deuterated (LxA4-d5), resolvin D1 (RvD1), resolvin D2 (RvD2), 7-maresin (7-MaR1),  
345 leukotriene B4 (LTB4), leukotriene B5 (LTB5), leukotriene B4 deuterated (LTB4-d4),  
346 10(S),17(S)-protectin (PDx), 18-hydroxyeicosapentaenoic acid (18-HEPE), dihydroxy-  
347 eicosatetraenoic acid (5,6-DiHETE), 15-hydroxyeicosatetraenoic acid (15-HETE) and 12-  
348 HETE, 8-HETE, 5-HETE, 5-HETE-d8, 17-hydroxy-docosahexaenoic acid (17-HDoHE) and  
349 14-HDoHE, 14,15-epoxyeicosatrienoic acid (14,15-EET) and 11,12-EET, 8,9-EET, 5,6- EET,  
350 5-oxoeicosatetraenoic acid (5-oxoETE) were purchased from Cayman Chemicals (Ann Arbor,  
351 MI, USA).

352

353 **Patients**

354 Patients (Table 1) were recruited from outpatient clinics of the Department of Medical and  
355 Surgical Sciences of the University of Bologna (Italy), and were included according to Rome  
356 III criteria for IBS. Healthy controls (HC) were asymptomatic subjects undergoing colonoscopy  
357 for colorectal cancer screening. In this group, we excluded subjects based on the presence of  
358 the following symptoms in the last 12 months: abdominal discomfort or pain, bloating, and  
359 bowel habit changes. Exclusion criteria for both IBS and HC included major abdominal surgery,  
360 any organic syndrome, celiac disease (excluded by detection of anti-transglutaminase and anti-  
361 endomysial antibodies), asthma, food allergy, or other allergic disorders. None of these patients  
362 or HC were taking nonsteroidal anti-inflammatory drugs or any other anti-inflammatory drugs  
363 (including steroids, antihistamines, and mast cell stabilizers). Patients and HC gave written



364 informed consent. The study protocol was approved by the local Ethic Committee  
365 (64/2004/O/Sper and EM14/2006/O) and conducted in accordance with the Declaration of  
366 Helsinki. Patients underwent colonoscopy and, in all cases, 6 mucosal biopsies were obtained  
367 from the proximal descending colon. One biopsy was sent to the pathology department for  
368 exclusion of microscopic colitis or other microscopic tissue abnormalities and 4 were used in  
369 other studies. One biopsy was snap-frozen in liquid nitrogen for lipid extraction and PUFA  
370 quantification for the purpose of our study.

371

### 372 **Lipid extraction**

373 Biopsies were crushed with a FastPrep®-24 Instrument (MP Biomedicals, Illkirch, France) in  
374 500 µL of Hank's balanced salt solution (HBSS, Invitrogen, Villebon sur Yvette, France) and 5  
375 µL of internal standard mixture (LxA4-d5, LTB4-d4 and 5-HETE-d8 at 400 ng/mL in MeOH).  
376 After 2 crush cycles (6.5 m/s, 30 s), 10 µL were withdrawn for protein quantification and 300  
377 µL of cold methanol were added. Samples were centrifuged at 1000 g for 15 min at 4 °C.  
378 Supernatants were collected, completed to 2 mL in H<sub>2</sub>O and submitted to solid-phase extraction  
379 using HRX-50 mg 96-well (Macherey Nagel, Hoerd, France). Briefly, after plate conditioning,  
380 the sample was loaded at flow rate of 0.1 mL/min. After complete loading, the plate was washed  
381 with H<sub>2</sub>O/MeOH (90:10, 2 mL) and lipid mediators were eluted with MeOH (2 mL). Solvent  
382 was evaporated under nitrogen and samples were dissolved with MeOH and stored at -80 °C  
383 for liquid chromatography/tandem mass spectrometry measurements.

384

### 385 **Liquid chromatography/tandem mass spectrometry (LC-MS/MS) measurements**

386 6kPGF1 $\alpha$ , TXB<sub>2</sub>, PGE<sub>2</sub>, PGA<sub>1</sub>, 8-isoPGA<sub>2</sub>, PGE<sub>3</sub>, 15d-PGJ<sub>2</sub>, LxA4, LxB4, RvD1, RvD2, 7-  
387 MaR1, LTB<sub>4</sub>, LTB<sub>5</sub>, PD<sub>x</sub>, 18-HEPE, 5,6-DiHETE, 15-HETE, 12-HETE, 8-HETE, 5-HETE,  
388 17-HDoHE, 14-HDoHE, 14,15-EET, 11,12-EET, 8,9-EET, 5,6-EET and 5-oxo-ETE were

389 quantified in human biopsies (57). To simultaneously separate 28 lipids of interest and 3  
390 deuterated internal standards, LC-MS/MS analysis was performed on ultra high performance  
391 liquid chromatography system (UHPLC, Agilent LC1290 Infinity) coupled to Agilent 6460  
392 triple quadrupole MS (Agilent Technologies) equipped with electro-spray ionization operating  
393 in negative mode. Reverse-phase UHPLC was performed using ZorBAX SB-C18 column  
394 (Agilent Technologies) with a gradient elution. The mobile phases consisted of water,  
395 acetonitrile (ACN) and formic acid (FA) (75:25:0.1; v/v/v) (A) and ACN, FA (100:0.1, v/v)  
396 (B). The linear gradient was as follows: 0% B at 0 min, 85% B at 8.5 min, 100% B at 9.5 min,  
397 100% B at 10.5 min and 0% B at 12 min. The flow rate was 0.35 mL/min. The autosampler was  
398 set at 5 °C and the injection volume was 5 µL. Data were acquired in Multiple Reaction  
399 Monitoring (MRM) mode with optimized conditions. Peak detection, integration and  
400 quantitative analysis were done using Mass Hunter Quantitative analysis software (Agilent  
401 Technologies). For each standard, calibration curves were built using 10 solutions at  
402 concentrations ranging from 0.95 ng/mL to 500 ng/mL. A linear regression with a weight factor  
403 of 1/X was applied for each compound. The limit of detection (LOD) and the limit of  
404 quantification (LOQ) were determined for the 28 compounds using signal to noise ratio (S/N).  
405 The LOD corresponded to the lowest concentration leading to a signal to noise over 3 and LOQ  
406 corresponded to the lowest concentration leading to a signal to noise over 10. All values under  
407 the LOQ were not considered. Blank samples were evaluated, and their injection showed no  
408 interference (no peak detected), during the analysis. Hierarchical clustering and heat-map were  
409 obtained with R ([www.r-project.org](http://www.r-project.org)). PUFA metabolite amounts were transformed to z-scores  
410 and clustered based on 1-Pearson correlation coefficient as distance and the Ward algorithm as  
411 agglomeration criterion.

412

413

414 **Animals**

415 C57BL/6 male mice (3 weeks-old) were purchased from Janvier (Le Genest Saint Isle, France).  
416 *Mrgprd*<sup>cre/+</sup> mice were a generous gift from Dr D. Anderson at Caltech Pasadena. These mice  
417 were previously generated by Rau et al 2009 (44) and were in an almost pure C57/Bl6J  
418 background when we received them at IBDM (Institut de Biologie du Développement de  
419 Marseille) mouse facility. There, the mice were kept as heterozygous and were backcrossed to  
420 C57/Bl6J for another 8 generations. *Mrgprd* deficient mice used in this study were obtained by  
421 intercrossing *Mrgprd*<sup>cre/+</sup> heterozygous mice. Animals were maintained in ventilated cages (4  
422 mice per cage) in a specific pathogen free room at 20–24 °C and relative humidity (40%–70%)  
423 with a 12 hours light/dark cycle and given free access to food and water. Animal Care and ethic  
424 Committee of US006/CREFE (CEEA-122) approved the whole study protocol (permit No.  
425 MP/01/64/09/12). *Mrgprd*<sup>EGFP</sup>-tagged mice (B6;129SP2-*Mrgprd*<sup>tm4.1(COP4)Mjz</sup>/Mmnc; MMRRC,  
426 North Carolina, USA) were raised and maintained at the University of Glasgow, and have been  
427 characterised previously (58). Experiments conducted at the University of Glasgow were  
428 approved by the University's Ethical Review Process Applications Panel, and were performed  
429 in accordance with the European Community directive 86/609/EC and the United Kingdom  
430 Animals (Scientific Procedures) Act 1986.

431

432 **Measurement of somatic nociception**

433 Paw-withdrawal thresholds were measured using calibrated von Frey filaments with forces  
434 ranging from 0.04 to 2 g (Stoelting, Wood Dale, IL, USA), which were applied onto the plantar  
435 surface of mice. Ascending series of von Frey filaments were applied with each monofilament  
436 being tested 5 times for approximately 1 second. Threshold to mechanical stimuli was  
437 calculated as the force value of the von Frey filament triggering 3 paw withdrawals over 5  
438 applications (59). Responses to mechanical stimuli were recorded before and 15 min, 30 min,

439 1 hour, 2 hours and 6 hours after an intraplantar injection of 0.1, 1, 10 or 100  $\mu\text{M}$  of 5-oxoETE  
440 or its vehicle (HBSS). In a second set of experiments, paw edema was measured using digital  
441 calipers (resolution 0.01; Mitutoyo, Aurora, IL, USA) at 1, 2, 3 and 4 hours after intraplantar  
442 injection of 100  $\mu\text{M}$  of 5-oxoETE. At the end of the experiment, paws were collected for  
443 histological analysis by hematoxylin and eosin staining (H&E).

444

#### 445 **Colorectal distension (CRD) and electromyography recordings**

446 Mice were administered either 100  $\mu\text{L}$  of 5-oxoETE (10  $\mu\text{M}$ ) or its vehicle (40% ethanol)  
447 intracolonicly. We performed a session of CRD and recorded visceromotor responses (VMR)  
448 from implanted electrodes before and 30 min after treatment as previously described (60). Data  
449 are presented as the difference between the VMR induced by the distension performed before  
450 and after intracolonic treatments. After distension, mouse colons were harvested to perform  
451 histological analysis (H&E) and myeloperoxidase activity assay.

452

#### 453 **Lumbar splanchnic nerve recording**

454 The distal colon with associated lumbar splanchnic nerves was removed from male C57BL/6  
455 mice (12 weeks). The colon was then opened along the anti-mesenteric border and pinned flat  
456 mucosal side up. The tissue was perfused (7 mL/min; 32-34  $^{\circ}\text{C}$ ) with carbogenated Krebs buffer  
457 (in mM: 124 NaCl; 4.8 KCl; 1.3  $\text{NaH}_2\text{PO}_4$ ; 2.4  $\text{CaCl}_2$ ; 1.2  $\text{MgSO}_4 \cdot 7\text{H}_2\text{O}$ ; 11.1 glucose; 25  
458  $\text{NaHCO}_3$ ) and supplemented with 10  $\mu\text{M}$  nifedipine and 10  $\mu\text{M}$  atropine to block smooth  
459 muscle contraction, and 3  $\mu\text{M}$  indomethacin to inhibit endogenous prostanoid production.  
460 Single unit activity was discriminated using wave form analysis software (Spike 2 Cambridge  
461 Electronic Design) from fibers teased from the lumbar splanchnic nerve (rostral to the inferior  
462 mesenteric ganglia), recorded using borosilicate glass suction electrodes. Signals were  
463 amplified, band pass filtered (gain 5K; 100-1300 Hz; Neurology, Digitiser Ltd, UK), digitally

464 filtered for 50Hz noise (Humbug, Quest Scientific, Canada), digitalised at 20 kHz (micro1401;  
465 Cambridge Electronic Design, UK) and displayed on a computer using Spike 2 software.  
466 Individual receptive fields of afferent nerve fibers were identified by systematically probing the  
467 tissue with a 1 g von Frey filament. Receptive fields that responded to probing and not to stretch  
468 were identified as serosal units (61). Once a serosal unit was identified a metal ring was placed  
469 over the receptive field and the baseline activity was observed for 3 min. The Krebs solution  
470 within the ring was then removed and replaced by 100  $\mu$ M 5-oxoETE pre-warmed to bath  
471 temperature. Following a 7 min challenge period the 5-oxoETE and ring were removed.

472

### 473 **Immunofluorescence in mouse colon**

474 The descending colons of 10 wild-type and 10 Mrgprd deficient mouse were cryoprotected in  
475 OCT compound, sectioned at a thickness of 10  $\mu$ m (one every 0.1 cm, 20 per mouse) on a  
476 cryostat (Leica CM1950, Nanterre, France), and mounted on Superfrost slides (Thermo Fisher  
477 Scientific, Villebonne-sur-Yvette, France). Slides were washed in phosphate buffered saline  
478 (PBS), 0.5% Triton X-100, and 1% bovine serum albumin (BSA) solution (Sigma, Saint-  
479 Quentin Fallavier, France) and incubated overnight at 4°C with the primary antibodies anti-  
480 Mrgprd (1:500, AMR-061, Alomone labs, Clinisciences, Nanterre, France) and anti-PGP9.5  
481 (1:500, AB86808, Abcam, Coger SAS, Paris, France). After washing, slides were incubated  
482 with the appropriate secondary antibody conjugated with Alexa Fluor® 488 or Alexa Fluor®  
483 555 (Thermo Fisher Scientific), washed, and mounted with ProLong Gold reagent containing  
484 DAPI (Molecular Probes). Images were acquired using Zeiss LSM-710 confocal microscopes  
485 (Carl Zeiss MicroImaging, Jena, Germany) with 20X objective in the inverted configuration.

486

### 487 **Single-cell qRT-PCR of retrogradely labelled mouse sensory neurons**

488 Dorsal root ganglia neurons projecting to the colon were selectively labelled, individually  
489 harvested by pulled glass pipette. After RNA extraction, single-cell RT-qPCR for the presence  
490 of *Mrgprd* mRNA transcripts was performed as previously described (62). In brief, adult mice  
491 were subjected to laparotomy under anesthesia and 6-8 injections of Fast Blue (~ 0.2  $\mu$ L, 2 %  
492 in saline; Polysciences GmbH) were made into the wall of the distal colon. Five days post-  
493 surgery, thoracolumbar (TL; T10-L1) DRG were collected and enzymatically dissociated (62).  
494 Individual cells were isolated by pulled glass pipette and collected into a preamplification  
495 mastermix containing 0.1  $\mu$ L SUPERase-in (Ambion, TX, USA), 0.2  $\mu$ L Superscript III Reverse  
496 Transcriptase/Platinum Taq mix (Invitrogen), 5  $\mu$ L CellDirect 2x reaction buffer (Invitrogen),  
497 2.5  $\mu$ L 0.2x primer/probe mix and 1.2  $\mu$ L TE buffer (Applichem, GmbH) before thermal cycling  
498 (50 °C for 30 min, 95 °C for 2 min, then 21 cycles of (95 °C for 15 seconds, 60 °C for 4 min)).  
499 TaqMan qPCR assays for *Mrgprd* (TaqMan Assay ID: Mm01701850\_s1) and *Trpv1*  
500 (Mm01246300\_m1) were performed on diluted cDNA products (1:5 in TE buffer) using the  
501 following cycling protocol: 50°C for 2 minutes, 95°C for 10 minutes, then 40 cycles of (95°C  
502 for 15 seconds, 60°C for 1 minutes. Glyceraldehyde-3-phosphate dehydrogenase (GAPDH)  
503 acted as an internal positive control and sample of the bath solution was used as a no-template  
504 negative control, with all single-cell RT-PCR products expressing GAPDH, whilst bath control  
505 samples did not. The quantitative assessment of gene expression was determined by  
506 quantification of cycle (Cq) values lower than the threshold of 35 that were considered as  
507 positive. In total, 15 single cells per spinal region (TL) per mouse (n=3) were isolated, therefore  
508 the expression of mRNA transcripts was determined in 45 colonic sensory neurons.

509

510 **Immunohistochemistry of Fast Blue-labelled colonic sensory neurons from *Mrgprd*<sup>EGFP</sup>**  
511 **tagged mice.**

512 From thoracolumbar regions, DRG T13 were stained from 4 *Mrgprd*<sup>EGFP</sup> mice retrogradely  
513 labelled with Fast Blue to the colon, as described above. A single T13 DRG was sectioned  
514 sequentially across 10 slides at 12 µm thickness. Therefore, on a given slide, the T13 DRG was  
515 sampled at 120 µm intervals for the full thickness of the DRG. In total 16 sections from 4  
516 animals were analysed, yielding 274 Fast Blue labelled cells. Slides were stained with chicken  
517 anti-GFP (1:1000; Abcam Ab13790) and rabbit anti-CGRP (1:10000, Sigma C8198) antisera.  
518 Secondary antibody used were goat anti-Chicken-488 (1:1000) and donkey anti-Rabbit-594  
519 (1:1000). Each probe (e.g. *Mrgprd*<sup>EGFP</sup> and CGRP) per section has a background reading  
520 subtracted and was normalised between the maximum and minimum intensity cells. A threshold  
521 of mean + 3 times SD for the minimum intensity cells (from all 16 sections) was used to  
522 differentiate positive from negative cells. Positive cells were then manually confirmed.

523

#### 524 **Ca<sup>2+</sup> imaging of mouse sensory neurons**

525 Dorsal root ganglia of wild-type and *Mrgprd* deficient mice were rinsed in cold HBSS  
526 (Invitrogen), and enzymatically dissociated as described previously (63). Neurons were plated  
527 in 96 wells plate (fluorescence Greiner bio one, Dominique Dutscher, Brumath, France) and  
528 cultured for 24 hours. In a first set of experiments, neurons were treated with 5-oxoETE (1, 5,  
529 25, 50 and 100 µM) or vehicle (HBSS). In a second set of experiments, neurons were incubated  
530 for 1 hour with 10 µg/mL of isolectin B4 from Griffonia simplicifolia conjugated to Alexa  
531 Fluor® 594 (ThermoFisher) in order to differentiate IB4-positive and -negative sensory  
532 neurons. Ca<sup>2+</sup> flux was monitored by recording changing emission intensity of Fluo-4  
533 (Molecular probe) following treatment with 5-oxoETE (10 µM) or its vehicle. In a third set of  
534 experiments, neurons were pre-incubated with pertussis toxin (PTX, 250 ng/mL) overnight or  
535 with the U73122 phospholipase C inhibitor (10 µM) 30 min, before treatment with 5-oxoETE  
536 (50 µM) or its vehicle.

537

### 538 **Expression of shRNA directed against *Mrgprd* in sensory neurons**

539 Lentiviral particles were produced as previously described (64). Briefly, HEK293T/17 cells  
540 were cultured according to supplier's recommendations (ATCC, USA).  $1.7 \times 10^7$  cells were  
541 seeded into a 175 cm<sup>2</sup> culture flask containing 30 mL of DMEM (Gibco, USA) and then  
542 incubated at 37°C 5% CO<sub>2</sub>. In the next day, cells were transfected with a mixture of structural  
543 (psPAX2 and pMD2.G; Addgene, Cambridge, MA, USA) and transfer vectors (shRNA  
544 *Mrgprd*-RFP-CB or the control shRNA-RFP-CB; OriGene Technologies, Rockville, USA), by  
545 using the transfection reagent GeneJuice (Millipore, USA). Cells were incubated overnight at  
546 37°C 5% CO<sub>2</sub>, then the medium was replaced by 18 mL of OptiMEM (Gibco, USA). Cell  
547 culture supernatants were harvested 48 h later, cleared by centrifugation and filtration with a  
548 0.45 µm syringe filter. Neurons plated in 96 wells plate coated with poly-L-ornithine/laminin  
549 and cultivated in Neurobasal medium supplemented with B27 and L-glutamine were transduced  
550 with 50 µL of lentivirus supernatant. Three days later, a transduction efficiency of 35 % was  
551 achieved and calcium flux assay was performed in response to 5-oxoETE (10 µM), as described  
552 above.

553

### 554 **Ca<sup>2+</sup> flux in CHO cells expressing *Mrgprd***

555 Mouse *Mrgprd*-expression plasmid (OriGene Technologies, Rockville, USA) was transfected  
556 into CHO cells using GeneJuice Transfection Reagent (1 µg of plasmid for 3 µL of GeneJuice).  
557 The cells were incubated in Ham's F12 Nutrient Mixture with 5% of FBS. G418 (Sigma) was  
558 used as the selection antibiotic.  $50 \times 10^3$  cells/well in a 96 wells plate were incubated with fluo-  
559 8 loading solution (Fluo-8-AM; Invitrogen) according to manufacturer's instructions. The  
560 fluorescence was then measured at 530 nm on a microplate reader (NOVOstar; BMG Labtech)  
561 for 1 min. Five seconds after the beginning of calcium measures, 5-oxoETE (1, 10, 25, 50, 100



562 and 200  $\mu$ M) or  $\beta$ -alanine (Sigma-Aldrich; 1 mM) was added. Data were collected and analyzed  
563 with the NOVOstar software.

564

### 565 **Ca<sup>2+</sup> imaging of human sensory neurons**

566 Experiments were conducted following the opinion number 14-164 of the institutional review  
567 board (IRB00003888) of French institute of medical research and health. Three human DRG  
568 T11 (thoracic position 11) were supplied through the national human tissue resource center  
569 from the national disease resource interchange (NDRI). DRG were received unfixed in DMEM  
570 at 4°C. DRG were dissected, minced in HBSS and incubated in Papain (27 $\mu$ g/mL) (Sigma,  
571 Saint Quentin Fallavier, France) for 20 min at 37°C. After a wash with L-15 Wash Buffer  
572 [Leibovitz's L-15 Medium (Invitrogen), 10% FBS (Invitrogen)] and HBSS, DRG were  
573 incubated in HBSS containing 1 mg/mL of collagenase type IV (Worthington, Lakewood, NJ,  
574 USA) and 4 mg/mL of dispase II (Sigma). L-15 Wash buffer was added to neutralize enzymatic  
575 activities and the suspension was centrifuged at 1000 g for 5 min. The cycle of digestion was  
576 repeated 3 times 15 min. Neurons in the pellet were suspended in Neurobasal medium  
577 (Invitrogen) containing 2% B27, 2 mmol/L glutamine, 1% penicillin/streptomycin and 10  $\mu$ M  
578 each of cytosine arabinoside, 5-Fluoro-2'-deoxyuridine (FUDR), Uridine (all from Sigma). The  
579 medium was changed every 3 days without cytosine arabinoside. Cells were plated in CC2  
580 LabTek II (Nunc, Dominique Dutscher, Brumath, France) for calcium signalling assay as  
581 described above in response to 5-oxoETE (0.1, 1 and 10  $\mu$ M) and immunocytochemistry.

582

### 583 **Immunofluorescence in human dorsal root ganglia**

584 Experiments were conducted following the opinion number 12-074 of the institutional review  
585 board (IRB00003888) of French institute of medical research and health. Two human DRG T11  
586 (thoracic position 11) were supplied through the national human tissue resource center from the

587 national disease resource interchange (NDRI). DRG were received unfixed and cryoprotected.  
588 DRG were cut into 20  $\mu\text{m}$  sections on a cryostat (Leica CM1950, Nanterre, France), and  
589 mounted on Superfrost slides (Thermo Fisher Scientific, Villebonne-sur-Yvette, France).  
590 Cultured sensory neurons and slides were washed in phosphate buffered saline (PBS), 0.5%  
591 Triton X-100, and 1% bovine serum albumin (BSA) solution (Sigma, Saint-Quentin Fallavier,  
592 France) and incubated overnight at 4°C with the anti-Mrgprd (1:100, LS-A4123, LifeSpan  
593 Biosciences, Clinisciences, Nanterre, France) and anti-PGP9.5 (1:500, AB86808, Abcam).  
594 After washing, slides and cultured DRG were incubated with the appropriate secondary  
595 antibody conjugated with Alexa Fluor 488 or Alexa Fluor 555, washed, and mounted with  
596 ProLong Gold reagent containing DAPI (Molecular Probes). Images were acquired using Zeiss  
597 LSM-710 confocal microscopes (Carl Zeiss MicroImaging, Jena, Germany) with 20X objective  
598 in the inverted configuration.

599

## 600 **Statistics**

601 Data are presented as means  $\pm$  standard error of the mean (SEM). Analyses were performed  
602 using GraphPad Prism 5.0 software (GraphPad, San Diego, CA). Comparisons between-groups  
603 were performed by Mann-Whitney test. Multiple comparisons within groups were performed  
604 by Kruskal-Wallis test, followed by Dunn's post-test. Statistical significance was accepted at P  
605  $< 0.05$ .

606

## 607 **Study approval**

608 The study protocol for biopsies collection was approved by the local Ethic Committee  
609 (64/2004/O/Sper and EM14/2006/O) and conducted in accordance with the Declaration of  
610 Helsinki. Patients and HC gave written informed consent. Fixed and fresh Human DRG were  
611 supplied through the national human tissue resource center from the national disease resource

612 interchange (NDRI, reference: DCEN1 001). Experiments on human DRG were conducted  
613 following the opinion number 14-164 of the institutional review board (IRB00003888) of  
614 French institute of medical research and health. Animal experiments were conducted following  
615 the European union council directive 2010/63/EU. Animal Care and ethic Committee of  
616 US006/CREFE (CEEA-122) approved the whole study protocol (permit No. MP/01/64/09/12).  
617 Experiments conducted at the University of Glasgow were approved by the University's Ethical  
618 Review Process Applications Panel, and were performed in accordance with the European  
619 Community directive 86/609/EC and the United Kingdom Animals (Scientific Procedures) Act  
620 1986.

621

## 622 **Supplementary Materials**

623 **Fig. S1:** Concentration of PUFA metabolites in biopsies of IBS patients

624 **Fig. S2:** Concentration of PUFA metabolites in biopsies of all IBS patients.

625 **Fig. S3:** 5-oxoETE does not induce somatic or visceral inflammation *in vivo*.

626 **Fig. S4:** Mrgprd immunoreactivity is observed in mouse colon

627 **Fig. S5:** Mrgprd immunoreactivity is not observed in colon of Mrgprd deficient mice.

628

629

630 References

- 631 1. F. Mearin, B. E. Lacy, L. Chang, W. D. Chey, A. J. Lembo, M. Simren, R. Spiller, Bowel  
632 Disorders. *Gastroenterology*, (2016).
- 633 2. P. Enck, Q. Aziz, G. Barbara, A. D. Farmer, S. Fukudo, E. A. Mayer, B. Niesler, E. M. Quigley, M.  
634 Rajilic-Stojanovic, M. Schemann, J. Schwillle-Kiuntke, M. Simren, S. Zipfel, R. C. Spiller,  
635 Irritable bowel syndrome. *Nat Rev Dis Primers* **2**, 16014 (2016).
- 636 3. L. Ohman, M. Simren, Pathogenesis of IBS: role of inflammation, immunity and neuroimmune  
637 interactions. *Nat Rev Gastroenterol Hepatol* **7**, 163-173 (2010).
- 638 4. N. Cenac, T. Bautzova, P. Le Faouder, N. A. Veldhuis, D. P. Poole, C. Rolland, J. Bertrand, W.  
639 Liedtke, M. Dubourdeau, J. Bertrand-Michel, L. Zecchi, V. Stanghellini, N. W. Bunnett, G.  
640 Barbara, N. Vergnolle, Quantification and Potential Functions of Endogenous Agonists of  
641 Transient Receptor Potential Channels in Patients With Irritable Bowel Syndrome.  
642 *Gastroenterology* **149**, 433-444 e437 (2015).
- 643 5. G. Barbara, B. Wang, V. Stanghellini, G. R. De, C. Cremon, N. G. Di, M. Trevisani, B. Campi, P.  
644 Geppetti, M. Tonini, N. W. Bunnett, D. Grundy, R. Corinaldesi, Mast cell-dependent excitation  
645 of visceral-nociceptive sensory neurons in irritable bowel syndrome. *Gastroenterology* **132**,  
646 26-37 (2007).
- 647 6. G. Clarke, S. M. O'Mahony, A. A. Hennessy, P. Ross, C. Stanton, J. F. Cryan, T. G. Dinan, Chain  
648 reactions: Early-life stress alters the metabolic profile of plasma polyunsaturated fatty acids  
649 in adulthood. *Behavioural Brain Research* **205**, 319-321 (2009).
- 650 7. G. Clarke, P. Fitzgerald, A. A. Hennessy, E. M. Cassidy, E. M. Quigley, P. Ross, C. Stanton, J. F.  
651 Cryan, T. G. Dinan, Marked elevations in pro-inflammatory polyunsaturated fatty acid  
652 metabolites in females with irritable bowel syndrome. *J.Lipid Res.* **51**, 1186-1192 (2010).
- 653 8. S. Tokuyama, K. Nakamoto, Unsaturated fatty acids and pain. *Biol Pharm Bull* **34**, 1174-1178  
654 (2011).
- 655 9. A. A. Berbert, C. R. Kondo, C. L. Almendra, T. Matsuo, I. Dichi, Supplementation of fish oil and  
656 olive oil in patients with rheumatoid arthritis. *Nutrition* **21**, 131-136 (2005).
- 657 10. P. C. Calder, Session 3: Joint Nutrition Society and Irish Nutrition and Dietetic Institute  
658 Symposium on 'Nutrition and autoimmune disease' PUFA, inflammatory processes and  
659 rheumatoid arthritis. *Proc Nutr Soc* **67**, 409-418 (2008).
- 660 11. Z. Harel, F. M. Biro, R. K. Kottenhahn, S. L. Rosenthal, Supplementation with omega-3  
661 polyunsaturated fatty acids in the management of dysmenorrhea in adolescents. *Am J Obstet*  
662 *Gynecol* **174**, 1335-1338 (1996).
- 663 12. A. Belluzzi, S. Boschi, C. Brignola, A. Munarini, G. Cariani, F. Miglio, Polyunsaturated fatty  
664 acids and inflammatory bowel disease. *Am J Clin Nutr* **71**, 339S-342S (2000).
- 665 13. D. Miyazawa, A. Ikemoto, Y. Fujii, H. Okuyama, Dietary alpha-linolenic acid suppresses the  
666 formation of lysophosphatidic acid, a lipid mediator, in rat platelets compared with linoleic  
667 acid. *Life Sci* **73**, 2083-2090 (2003).
- 668 14. C. Ramsden, C. Gagnon, J. Graciosa, K. Faurot, R. David, J. A. Bralley, R. N. Harden, Do omega-  
669 6 and trans fatty acids play a role in complex regional pain syndrome? A pilot study. *Pain*  
670 *Med* **11**, 1115-1125 (2010).
- 671 15. A. M. Patwardhan, P. E. Scotland, A. N. Akopian, K. M. Hargreaves, Activation of TRPV1 in the  
672 spinal cord by oxidized linoleic acid metabolites contributes to inflammatory hyperalgesia.  
673 *Proc Natl Acad Sci U S A* **106**, 18820-18824 (2009).
- 674 16. J. Y. Lim, C. K. Park, S. W. Hwang, Biological Roles of Resolvins and Related Substances in the  
675 Resolution of Pain. *Biomed Res Int* **2015**, 830930 (2015).
- 676 17. Z. Z. Xu, L. Zhang, T. Liu, J. Y. Park, T. Berta, R. Yang, C. N. Serhan, R. R. Ji, Resolvins RvE1 and  
677 RvD1 attenuate inflammatory pain via central and peripheral actions. *Nat Med* **16**, 592-597,  
678 591p following 597 (2010).

- 679 18. S. Bang, S. Yoo, T. J. Yang, H. Cho, Y. G. Kim, S. W. Hwang, Resolvin D1 attenuates activation  
680 of sensory transient receptor potential channels leading to multiple anti-nociception. *Br J*  
681 *Pharmacol* **161**, 707-720 (2010).
- 682 19. C. K. Park, Z. Z. Xu, T. Liu, N. Lu, C. N. Serhan, R. R. Ji, Resolvin D2 is a potent endogenous  
683 inhibitor for transient receptor potential subtype V1/A1, inflammatory pain, and spinal cord  
684 synaptic plasticity in mice: distinct roles of resolvin D1, D2, and E1. *J Neurosci* **31**, 18433-  
685 18438 (2011).
- 686 20. C. K. Park, Maresin 1 Inhibits TRPV1 in Temporomandibular Joint-Related Trigeminal  
687 Nociceptive Neurons and TMJ Inflammation-Induced Synaptic Plasticity in the Trigeminal  
688 Nucleus. *Mediators Inflamm* **2015**, 275126 (2015).
- 689 21. H. Harizi, J. B. Corcuff, N. Gualde, Arachidonic-acid-derived eicosanoids: roles in biology and  
690 immunopathology. *Trends Mol.Med.* **14**, 461-469 (2008).
- 691 22. G. A. Higgs, S. Moncada, J. R. Vane, Eicosanoids in inflammation. *Ann Clin Res* **16**, 287-299  
692 (1984).
- 693 23. L. W. Fu, J. C. Longhurst, Bradykinin and thromboxane A2 reciprocally interact to  
694 synergistically stimulate cardiac spinal afferents during myocardial ischemia. *Am J Physiol*  
695 *Heart Circ Physiol* **298**, H235-244 (2010).
- 696 24. J. C. Longhurst, R. A. Benham, S. V. Rendig, Increased concentration of leukotriene B4 but not  
697 thromboxane B2 in intestinal lymph of cats during brief ischemia. *Am J Physiol* **262**, H1482-  
698 1485 (1992).
- 699 25. S. Zhang, G. Grabauskas, X. Wu, M. K. Joo, A. Heldsinger, I. Song, C. Owyang, S. Yu, Role of  
700 prostaglandin D2 in mast cell activation-induced sensitization of esophageal vagal afferents.  
701 *Am J Physiol Gastrointest Liver Physiol* **304**, G908-916 (2013).
- 702 26. M. S. Gold, L. Zhang, D. L. Wrigley, R. J. Traub, Prostaglandin E(2) modulates TTX-R I(Na) in rat  
703 colonic sensory neurons. *J Neurophysiol* **88**, 1512-1522 (2002).
- 704 27. C. I. Svensson, M. Zattoni, C. N. Serhan, Lipoxins and aspirin-triggered lipoxin inhibit  
705 inflammatory pain processing. *J Exp Med* **204**, 245-252 (2007).
- 706 28. M. J. Zylka, F. L. Rice, D. J. Anderson, Topographically distinct epidermal nociceptive circuits  
707 revealed by axonal tracers targeted to Mrgprd. *Neuron* **45**, 17-25 (2005).
- 708 29. M. W. Buczynski, D. S. Dumlao, E. A. Dennis, Thematic Review Series: Proteomics. An  
709 integrated omics analysis of eicosanoid biology. *J Lipid Res* **50**, 1015-1038 (2009).
- 710 30. R. R. Ji, Z. Z. Xu, G. Strichartz, C. N. Serhan, Emerging roles of resolvins in the resolution of  
711 inflammation and pain. *Trends Neurosci* **34**, 599-609 (2011).
- 712 31. A. E. Barden, M. Moghaddami, E. Mas, M. Phillips, L. G. Cleland, T. A. Mori, Specialised pro-  
713 resolving mediators of inflammation in inflammatory arthritis. *Prostaglandins Leukot Essent*  
714 *Fatty Acids* **107**, 24-29 (2016).
- 715 32. W. S. Powell, J. Rokach, Biosynthesis, biological effects, and receptors of  
716 hydroxyeicosatetraenoic acids (HETEs) and oxoeicosatetraenoic acids (oxo-ETEs) derived  
717 from arachidonic acid. *Biochim Biophys Acta* **1851**, 340-355 (2015).
- 718 33. W. S. Powell, F. Gravelle, S. Gravel, Metabolism of 5(S)-hydroxy-6,8,11,14-eicosatetraenoic  
719 acid and other 5(S)-hydroxyeicosanoids by a specific dehydrogenase in human  
720 polymorphonuclear leukocytes. *J Biol Chem* **267**, 19233-19241 (1992).
- 721 34. W. S. Powell, F. Gravelle, S. Gravel, Phorbol myristate acetate stimulates the formation of 5-  
722 oxo-6,8,11,14-eicosatetraenoic acid by human neutrophils by activating NADPH oxidase. *J*  
723 *Biol Chem* **269**, 25373-25380 (1994).
- 724 35. Y. Zhang, A. Styhler, W. S. Powell, Synthesis of 5-oxo-6,8,11,14-eicosatetraenoic acid by  
725 human monocytes and lymphocytes. *J Leukoc Biol* **59**, 847-854 (1996).
- 726 36. U. Zimpfer, S. Dichmann, C. C. Termeer, J. C. Simon, J. M. Schroder, J. Norgauer, Human  
727 dendritic cells are a physiological source of the chemotactic arachidonic acid metabolite 5-  
728 oxo-eicosatetraenoic acid. *Inflamm Res* **49**, 633-638 (2000).

- 729 37. K. R. Erlemann, C. Cossette, S. Gravel, A. Lesimple, G. J. Lee, G. Saha, J. Rokach, W. S. Powell,  
730 Airway epithelial cells synthesize the lipid mediator 5-oxo-ETE in response to oxidative stress.  
731 *Free Radic Biol Med* **42**, 654-664 (2007).
- 732 38. P. B. Stamatou, C. C. Chan, G. Monneret, D. Ethier, J. Rokach, W. S. Powell, 5-oxo-6,8,11,14-  
733 eicosatetraenoic acid stimulates the release of the eosinophil survival factor  
734 granulocyte/macrophage colony-stimulating factor from monocytes. *J Biol Chem* **279**, 28159-  
735 28164 (2004).
- 736 39. M. Guilbert, C. Ferland, M. Bosse, N. Flamand, S. Lavigne, M. Laviolette, 5-Oxo-6,8,11,14-  
737 eicosatetraenoic acid induces important eosinophil transmigration through basement  
738 membrane components: comparison of normal and asthmatic eosinophils. *Am J Respir Cell*  
739 *Mol Biol* **21**, 97-104 (1999).
- 740 40. G. E. Grant, J. Rokach, W. S. Powell, 5-Oxo-ETE and the OXE receptor. *Prostaglandins Other*  
741 *Lipid Mediat* **89**, 98-104 (2009).
- 742 41. E. Kocak, E. Akbal, S. Koklu, B. Ergul, M. Can, The Colonic Tissue Levels of TLR2, TLR4 and  
743 Nitric Oxide in Patients with Irritable Bowel Syndrome. *Intern Med* **55**, 1043-1048 (2016).
- 744 42. T. Shinohara, M. Harada, K. Ogi, M. Maruyama, R. Fujii, H. Tanaka, S. Fukusumi, H. Komatsu,  
745 M. Hosoya, Y. Noguchi, T. Watanabe, T. Moriya, Y. Itoh, S. Hinuma, Identification of a G  
746 protein-coupled receptor specifically responsive to beta-alanine. *J Biol Chem* **279**, 23559-  
747 23564 (2004).
- 748 43. D. J. Cavanaugh, H. Lee, L. Lo, S. D. Shields, M. J. Zylka, A. I. Basbaum, D. J. Anderson, Distinct  
749 subsets of unmyelinated primary sensory fibers mediate behavioral responses to noxious  
750 thermal and mechanical stimuli. *Proc Natl Acad Sci U S A* **106**, 9075-9080 (2009).
- 751 44. K. K. Rau, S. L. McIlwrath, H. Wang, J. J. Lawson, M. P. Jankowski, M. J. Zylka, D. J. Anderson,  
752 H. R. Koerber, Mrgprd enhances excitability in specific populations of cutaneous murine  
753 polymodal nociceptors. *J Neurosci* **29**, 8612-8619 (2009).
- 754 45. J. Zhang, D. J. Cavanaugh, M. I. Nemenov, A. I. Basbaum, The modality-specific contribution  
755 of peptidergic and non-peptidergic nociceptors is manifest at the level of dorsal horn  
756 nociceptive neurons. *J Physiol* **591**, 1097-1110 (2013).
- 757 46. Q. Liu, P. Sikand, C. Ma, Z. Tang, L. Han, Z. Li, S. Sun, R. H. LaMotte, X. Dong, Mechanisms of  
758 itch evoked by beta-alanine. *J Neurosci* **32**, 14532-14537 (2012).
- 759 47. S. K. Ajit, M. H. Pausch, J. D. Kennedy, E. J. Kaftan, Development of a FLIPR assay for the  
760 simultaneous identification of MrgD agonists and antagonists from a single screen. *J Biomed*  
761 *Biotechnol* **2010**, (2010).
- 762 48. J. A. Christianson, R. J. Traub, B. M. Davis, Differences in spinal distribution and  
763 neurochemical phenotype of colonic afferents in mouse and rat. *J Comp Neurol* **494**, 246-259  
764 (2006).
- 765 49. D. R. Robinson, P. A. McNaughton, M. L. Evans, G. A. Hicks, Characterization of the primary  
766 spinal afferent innervation of the mouse colon using retrograde labelling. *Neurogastroenterol*  
767 *Motil* **16**, 113-124 (2004).
- 768 50. J. R. Hockley, G. Boundouki, V. Cibert-Goton, C. McGuire, P. K. Yip, C. Chan, M. Tranter, J. N.  
769 Wood, M. A. Nassar, L. A. Blackshaw, Q. Aziz, G. J. Michael, M. D. Baker, W. J. Winchester, C.  
770 H. Knowles, D. C. Bulmer, Multiple roles for NaV1.9 in the activation of visceral afferents by  
771 noxious inflammatory, mechanical, and human disease-derived stimuli. *Pain* **155**, 1962-1975  
772 (2014).
- 773 51. J. R. F. Hockley, T. S. Taylor, G. Callejo, A. L. Wilbrey, A. Gutteridge, K. Bach, W. J. Winchester,  
774 D. C. Bulmer, G. McMurray, E. S. J. Smith, Single-cell RNAseq reveals seven classes of colonic  
775 sensory neuron. *Gut*, (2018).
- 776 52. R. A. Crozier, S. K. Ajit, E. J. Kaftan, M. H. Pausch, MrgD activation inhibits KCNQ/M-currents  
777 and contributes to enhanced neuronal excitability. *J Neurosci* **27**, 4492-4496 (2007).
- 778 53. G. Blackburn-Munro, B. S. Jensen, The anticonvulsant retigabine attenuates nociceptive  
779 behaviours in rat models of persistent and neuropathic pain. *Eur J Pharmacol* **460**, 109-116  
780 (2003).

- 781 54. G. M. Passmore, A. A. Selyanko, M. Mistry, M. Al-Qatari, S. J. Marsh, E. A. Matthews, A. H.  
782 Dickenson, T. A. Brown, S. A. Burbidge, M. Main, D. A. Brown, KCNQ/M currents in sensory  
783 neurons: significance for pain therapy. *J Neurosci* **23**, 7227-7236 (2003).
- 784 55. K. Hirano, K. Kuratani, M. Fujiyoshi, N. Tashiro, E. Hayashi, M. Kinoshita, Kv7.2-7.5 voltage-  
785 gated potassium channel (KCNQ2-5) opener, retigabine, reduces capsaicin-induced visceral  
786 pain in mice. *Neurosci Lett* **413**, 159-162 (2007).
- 787 56. M. Peiris, J. R. Hockley, D. E. Reed, E. S. J. Smith, D. C. Bulmer, L. A. Blackshaw, Peripheral KV7  
788 channels regulate visceral sensory function in mouse and human colon. *Mol Pain* **13**,  
789 1744806917709371 (2017).
- 790 57. P. Le Faouder, V. Baillif, I. Spreadbury, J. P. Motta, P. Rousset, G. Chene, C. Guigne, F. Terce,  
791 S. Vanner, N. Vergnolle, J. Bertrand-Michel, M. Dubourdeau, N. Cenac, LC-MS/MS method for  
792 rapid and concomitant quantification of pro-inflammatory and pro-resolving polyunsaturated  
793 fatty acid metabolites. *J Chromatogr B Analyt Technol Biomed Life Sci* **932**, 123-133 (2013).
- 794 58. H. Wang, M. J. Zylka, Mrgprd-expressing polymodal nociceptive neurons innervate most  
795 known classes of substantia gelatinosa neurons. *J Neurosci* **29**, 13202-13209 (2009).
- 796 59. L. Basso, J. Boue, K. Mahiddine, C. Blanpied, S. Robiou-du-Pont, N. Vergnolle, C. Deraison, G.  
797 Dietrich, Endogenous analgesia mediated by CD4(+) T lymphocytes is dependent on  
798 enkephalins in mice. *J Neuroinflammation* **13**, 132 (2016).
- 799 60. J. Boue, L. Basso, N. Cenac, C. Blanpied, M. Rolli-Derkinderen, M. Neunlist, N. Vergnolle, G.  
800 Dietrich, Endogenous regulation of visceral pain via production of opioids by colitogenic  
801 CD4(+) T cells in mice. *Gastroenterology* **146**, 166-175 (2014).
- 802 61. S. M. Brierley, R. C. Jones, 3rd, G. F. Gebhart, L. A. Blackshaw, Splanchnic and pelvic  
803 mechanosensory afferents signal different qualities of colonic stimuli in mice.  
804 *Gastroenterology* **127**, 166-178 (2004).
- 805 62. J. R. Hockley, M. M. Tranter, C. McGuire, G. Boundouki, V. Cibert-Goton, M. A. Thaha, L. A.  
806 Blackshaw, G. J. Michael, M. D. Baker, C. H. Knowles, W. J. Winchester, D. C. Bulmer, P2Y  
807 Receptors Sensitize Mouse and Human Colonic Nociceptors. *J Neurosci* **36**, 2364-2376 (2016).
- 808 63. N. Cenac, M. Castro, C. Desormeaux, P. Colin, M. Sie, M. Ranger, N. Vergnolle, A novel orally  
809 administered trimebutine compound (GIC-1001) is anti-nociceptive and features peripheral  
810 opioid agonistic activity and Hydrogen Sulphide-releasing capacity in mice. *Eur J Pain* **20**, 723-  
811 730 (2016).
- 812 64. A. Denadai-Souza, C. M. Ribeiro, C. Rolland, A. Thouard, C. Deraison, C. Scavone, D. Gonzalez-  
813 Dunia, N. Vergnolle, M. C. W. Avellar, Effect of tryptase inhibition on joint inflammation: a  
814 pharmacological and lentivirus-mediated gene transfer study. *Arthritis Res Ther* **19**, 124  
815 (2017).
- 816
- 817
- 818

819 **Acknowledgments:** The authors thank the microscope core facility, INSERM UMR1043,  
820 Toulouse, the animal care facility, Genetoul, anexplor, US006/INSERM, Toulouse and the  
821 animal experiment platform of Toxalim (Research Centre in Food Toxicology), Toulouse  
822 University, INRA, ENVT, INP-Purpan, UPS, Toulouse, for their technical support. The authors  
823 acknowledge the National Diseases Research Interchange (NDRI) for supplying the human  
824 DRG. Lipidomic analyses were performed on the Toulouse INSERM Metatoul-Lipidomique  
825 Core Facility-MetaboHub ANR-11-INBS-010. Mrgprd deficient mice were a generous gift  
826 from David J Anderson (Caltech). **Funding:** Alexandre Denadai-Souza was recipient of a post-  
827 doctoral fellowship from São Paulo Research Foundation (FAPESP; process 2012/07784-4).  
828 Giovanni Barbara is a recipient of an educational grant from Fondazione del Monte di Bologna  
829 e Ravenna, Bologna, Italy. This work was supported by the Agence Nationale de la Recherche  
830 (to Nicolas Cenac), the Region Midi-Pyrénées (to Pauline Le Faouder and Nicolas Cenac), the  
831 Italian Ministry of Education, University and Research (No. 2002052573 and No. 2007Z292XF  
832 and 2009MFSXNZ) and funds from the University of Bologna (to Giovanni Barbara), funds  
833 from Bowel and Cancer Research (to Michael M. Tranter), BBSRC (BB/P007996/1 to David I  
834 Hughes, and BB/R006210/1 to James R F Hockley and Ewan St John Smith), a Rosetrees  
835 Postdoctoral Grant (A1296) awarded to James R F Hockley and Ewan St John Smith, and a  
836 European Research Council (ERC) grant to Nathalie Vergnolle (ERC-2012-StG-20111109).  
837 This work was also supported by the platform Aninfimip, an EquipEx ('Equipement  
838 d'Excellence') supported by the French government through the Investments for the Future  
839 program (ANR-11-EQPX-0003). **Author contributions:** TB, TPB and JRFH: design research  
840 studies, conduct experiments, acquire and analyze data. MMT, MRB, PLF, JP and CD: acquire  
841 and analyze data. LB, CR and ADS: conduct experiments. AM, PM and DIH: raised the  
842 different genetically modified mice and participate to the revision of the manuscript. EJS:  
843 participate to the revision of the manuscript. NV, AM, HE and GD: write the manuscript. GB:  
844 conduct experiments and write the manuscript. DB: conduct experiments, analyze data and  
845 write the manuscript. NC: design research studies, conduct experiments, acquire data, analyze  
846 data and write the manuscript. **Competing interests:** The authors have declared that no conflict  
847 of interest exists.

848

849



850 **Table 1:** Characteristics of patients from which biopsies were collected for PUFA metabolites  
 851 quantification

	<b>Control</b>	<b>IBS</b>
<b>Number</b>	14	50
<b>Age</b>	49 (20-76)	43 (20-72)
<b>Sex ratio (F/M)</b>	8/6	32/18
<b>Bowel movements:</b>		
Diarrhea	0	20
Constipation	0	20
Mix	0	10

852

853

854 **Table 2:** Percentage of fast-blue positive neurons expressing Mrgprd, CGRP or both per  
 855 Mrgprd-GFP mouse DRG T13

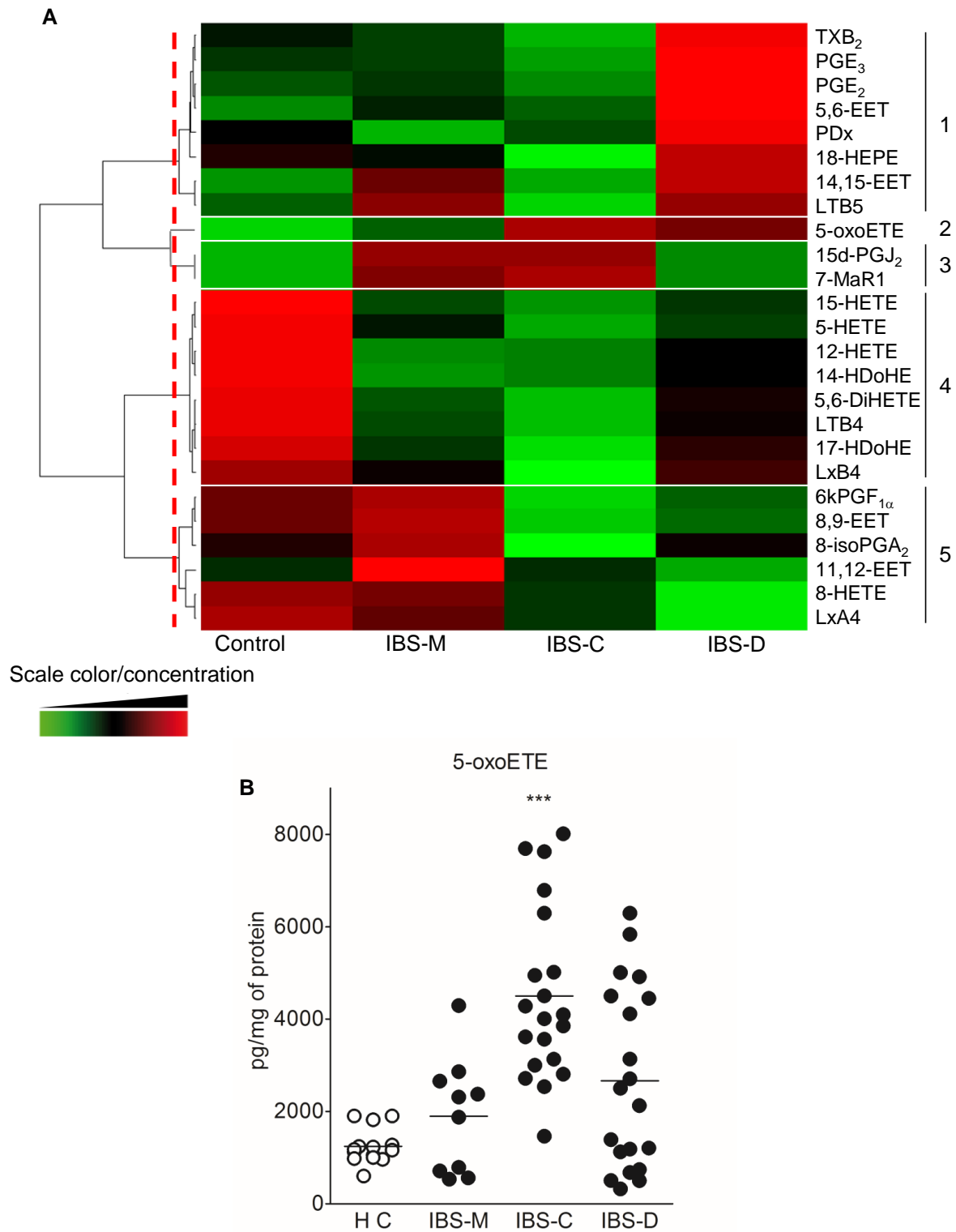
<b>Animal</b>	<b>Mrgprd+</b>	<b>CGRP+</b>	<b>Mrgprd+ &amp; CGRP+</b>
<b>A</b>	9 / 75 (12.0%)	54 / 75 (72.0%)	0 / 75 (0.0%)
<b>B</b>	2 / 38 (5.3%)	24 / 38 (63.2%)	0 / 38 (0.0%)
<b>C</b>	10 / 101 (9.9%)	64 / 101 (63.4%)	1 / 101 (1.0%)
<b>D</b>	1 / 60 (1.7%)	46 / 60 (76.7%)	0 / 60 (0.0%)
<b>Total (mean ± SD)</b>	7.2 ± 4.6 %	68.8 ± 6.7 %	0.3 ± 0.5 %

856

857

858

Figure 1



859

860 **Fig.1: Quantification of PUFA metabolites in mucosa of IBS patients.** A Heat-map of PUFA

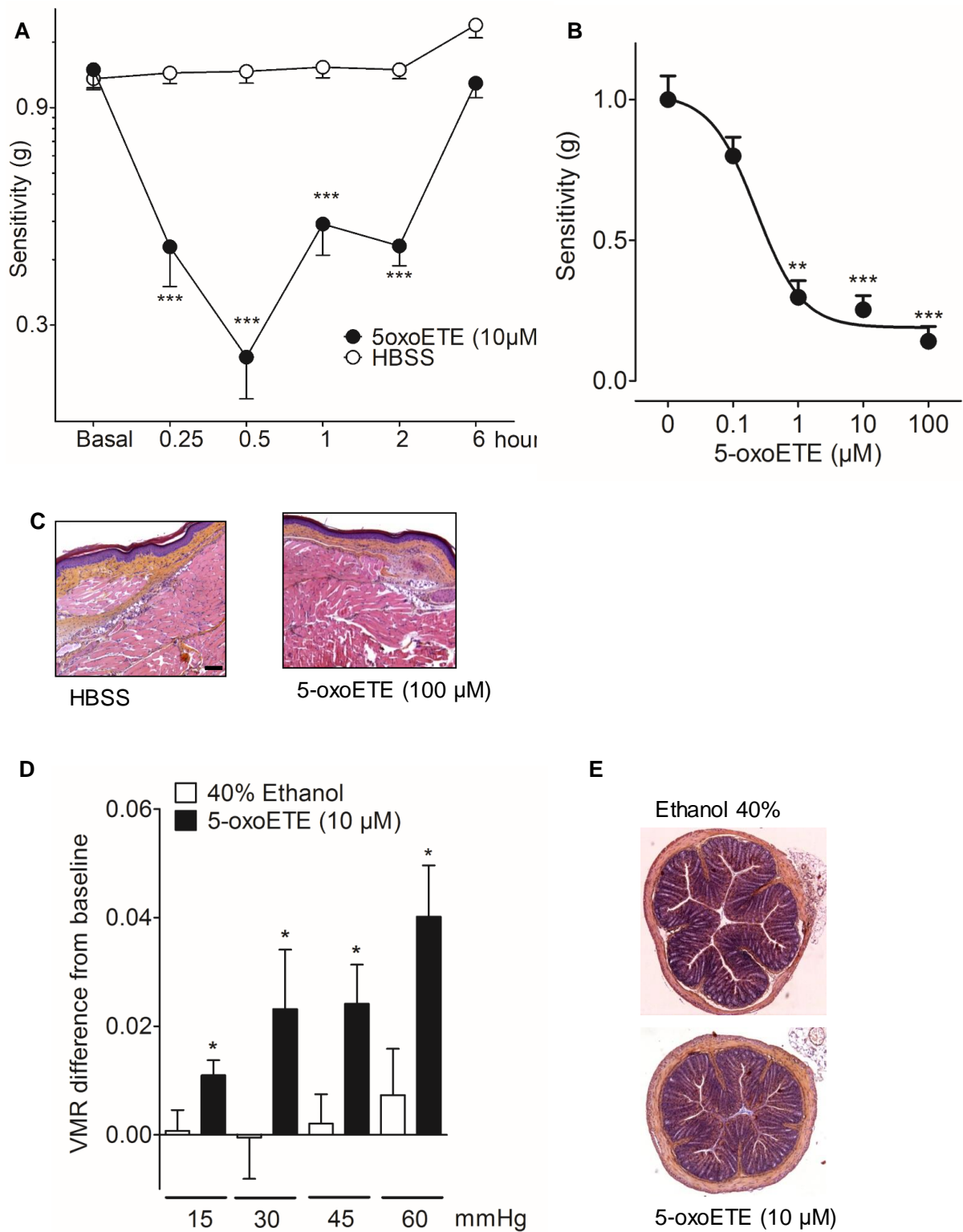
861 metabolites quantified by liquid chromatography-tandem mass spectrometry. Data are shown

862 in a matrix format: each row represents a single PUFA metabolite, and each column represents

863 a subgroup of patients. Each color patch represents the normalized quantity of PUFA  
864 metabolites (row) in a subgroup of patients (column), with a continuum of quantity from bright  
865 green (lowest) to bright red (highest). The pattern and length of the branches in the dendrograms  
866 reflect the relatedness of the PUFA metabolites. The dashed red line is the dendrogram distance  
867 used to cluster PUFA metabolites. **B** 5-oxoETE quantified by liquid chromatography-tandem  
868 mass spectrometry in mucosa of healthy control (white circle) and IBS (black circle). Data are  
869 expressed in pg/mg protein and represented as mean  $\pm$  SEM of 10 to 20 biopsies per group.  
870 Statistical analysis was performed using Kruskal-Wallis analysis of variance and subsequent  
871 Dunn's post hoc test. \*\*\*  $p < 0.001$ , significantly different from healthy control group.

872

**Figure 2**



873

874 **Fig.2: 5-oxoETE induces somatic and visceral hypersensitivity *in vivo*.** Mice were

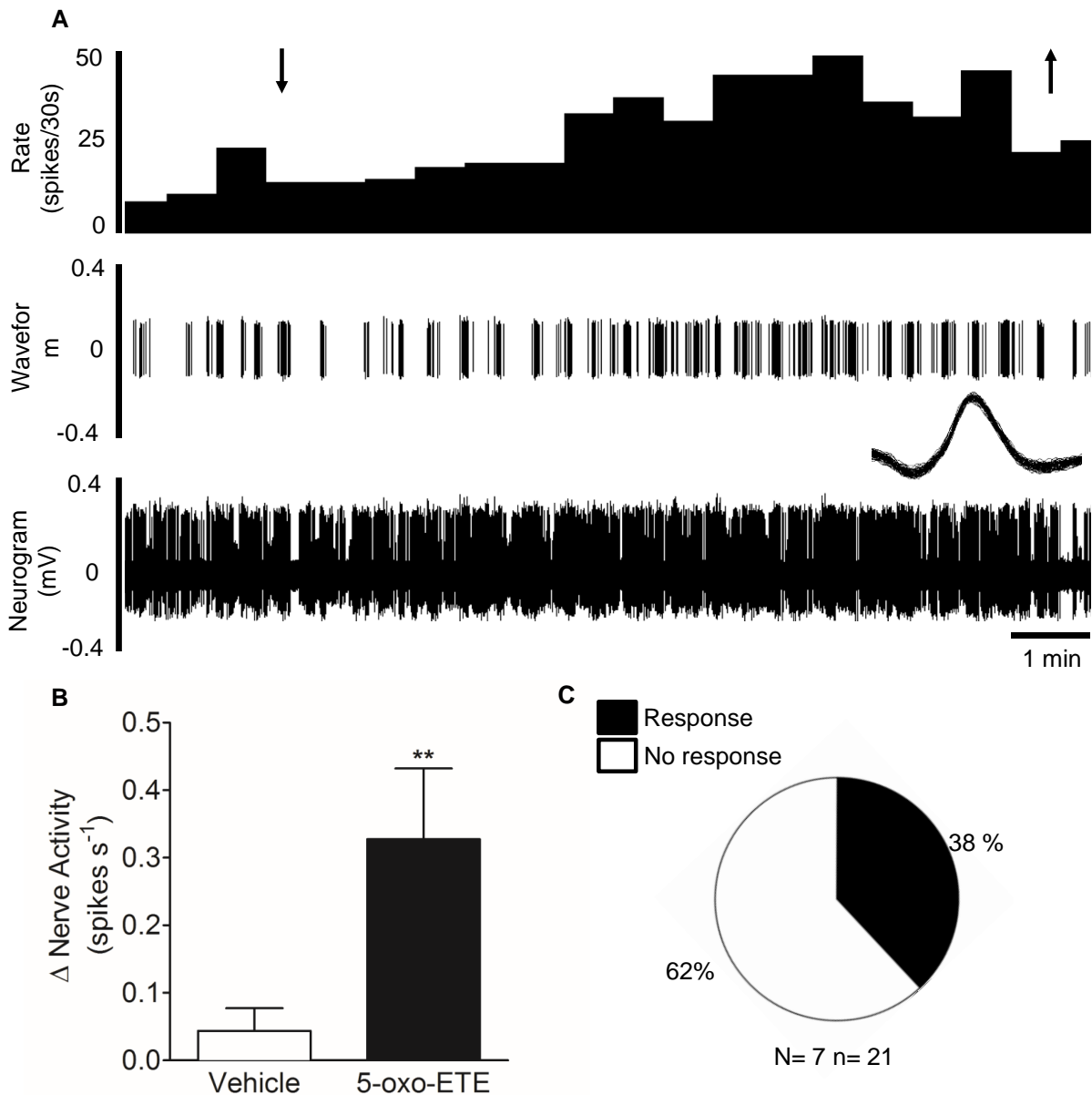
875 subcutaneously injected with either HBSS (white circle) or 5-oxoETE (black circle) into hind

876 footpads. **A** Somatic pain monitored using the von Frey test at different times (15 and 30 min,

877 1, 2 and 6 hours) following 5-oxoETE (10  $\mu$ M) injection; n=3 independent experiments of 5  
878 mice per groups. **B** Von Frey test performed 30 min after injection of 5-oxoETE at different  
879 concentrations (0.1, 1, 10 or 100  $\mu$ M); n=2 experiments of 6 mice per group. Data are expressed  
880 as mean  $\pm$  SEM. **C** Mouse paw tissue samples stained with H&E 6 h after administration of  
881 HBSS (left panel) or 5-oxoETE (100  $\mu$ M) (right panel). **D** Visceromotor response (VMR) to  
882 increasing pressures of colorectal distension before and 30 min after intracolonic administration  
883 of 5-oxoETE (10 $\mu$ M; black bars) or vehicle (40% ethanol; white bars); n=2 experiments of 10  
884 mice per group. Data are expressed as mean  $\pm$  SEM relative to the baseline recorded before  
885 treatment. **E** Colon tissue samples stained with H&E from 40% ethanol treated-mice (1 hour)  
886 (upper panel) or 5-oxoETE-treated mice (10  $\mu$ M; 1 hour) (lower panel). Statistical analysis was  
887 performed using Kruskal-Wallis analysis of variance and subsequent Dunn's post hoc test. \*\*  
888 p<0.01, \*\*\* p<0.001, significantly different from control mice.

889

Figure 3



890

891 **Fig.3: 5-oxoETE induces lumbar splanchnic nerve firing.** **A** Example of multi-unit recording

892 showing lumbar splanchnic (i.e. colon-innervating) nerve response to ring application (7 min)

893 of 5-oxoETE in mouse serosal afferents. Arrows indicate application and removal of 5-oxoETE.

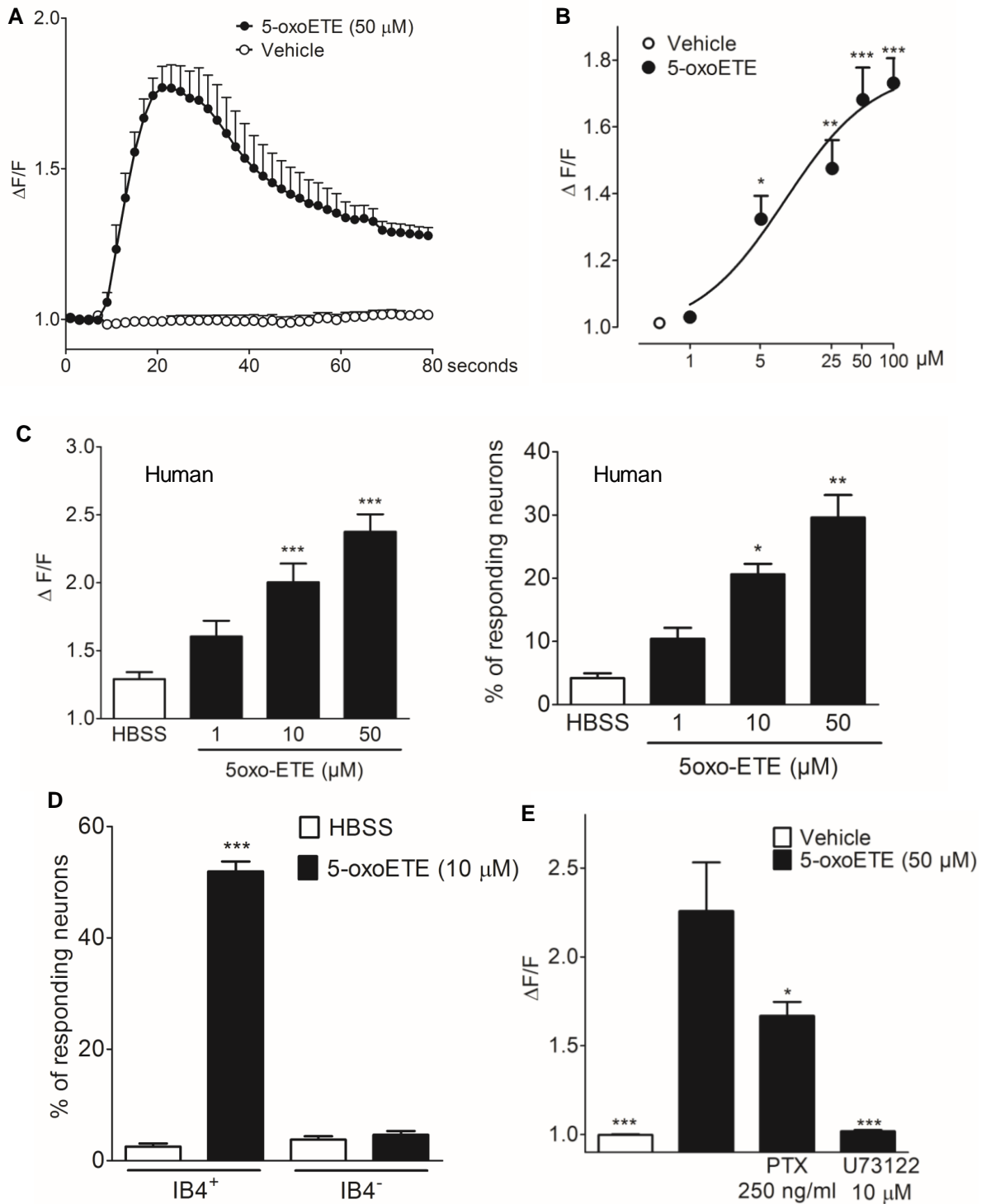
894 **B** Mean change in firing/second in serosal and mesenteric receptive fields compared with

895 vehicle response of Krebs buffer. Statistical analysis was performed using Mann-Whitney t-

896 test. \*\*  $p < 0.01$ , significantly different from vehicle. **C** Proportion of responses in lumbar

897 splanchnic afferents to application of 5-oxoETE.

**Figure 4**



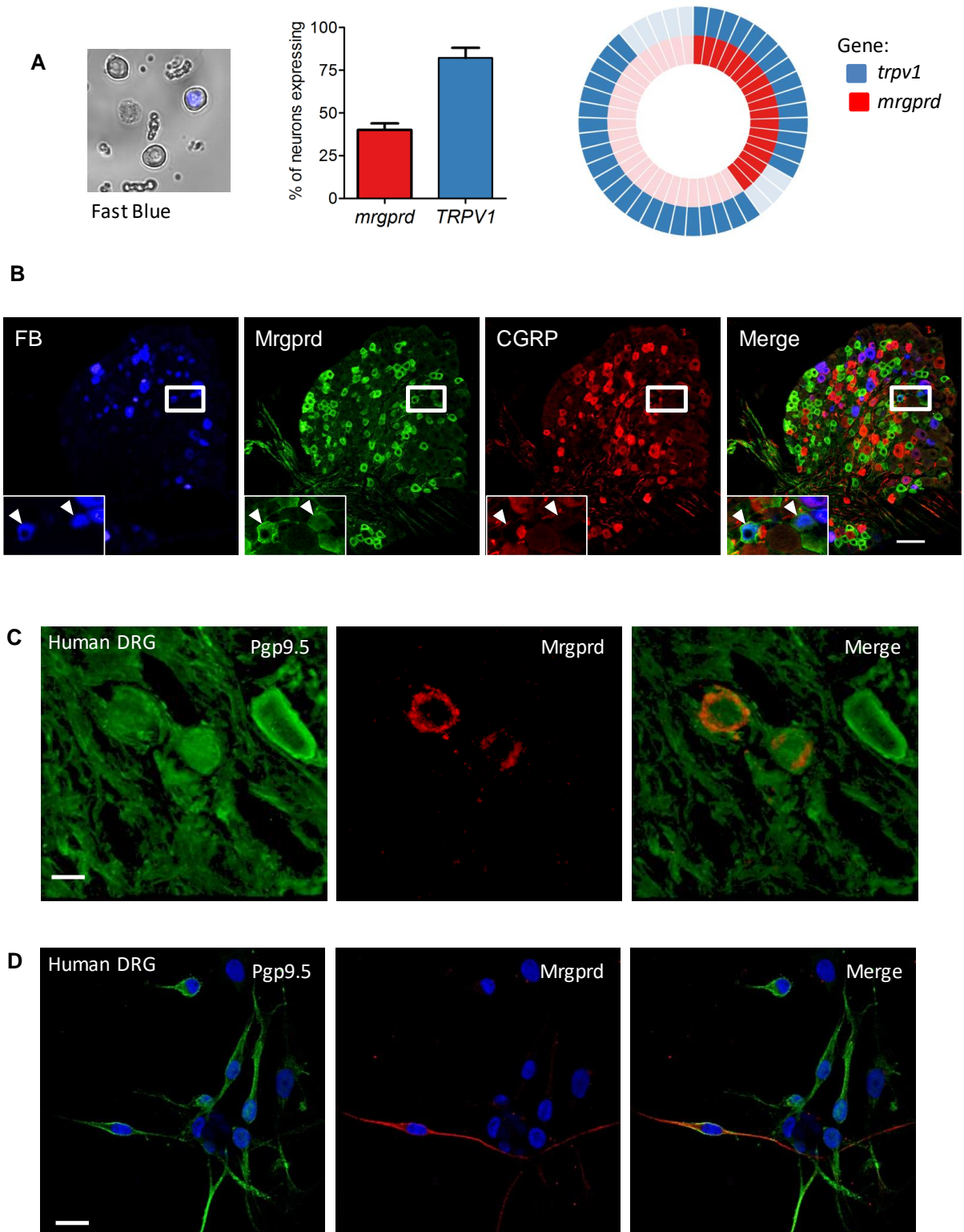
898

899 **Fig.4: 5-oxoETE induces an increase in  $[Ca^{2+}]$  in sensory neurons via a GPCR. A**  
 900 **Representative trace of  $Ca^{2+}$  flux experiments in sensory neurons performed without  $Ca^{2+}/Mg^{2+}$**   
 901 **in the extracellular medium and exposed to 5-oxoETE (50  $\mu$ M) or its vehicle (HBSS). B  $Ca^{2+}$**   
 902 **flux in mouse sensory neurons exposed to increasing amounts of 5-oxoETE (black circle) or**

903 vehicle (HBSS; white circle); n=7 independent experiments of 3 wells per condition and 60 to  
904 80 neurons per well. **C** Amplitude of  $[Ca^{2+}]_i$  ( $\Delta F/F$ ; left panel) in human sensory neurons and  
905 percentage of responding neurons (right panel) exposed to increasing amounts of 5-oxoETE  
906 (black bar) or vehicle (HBSS; white bar); n=3 independent experiments of 3 wells per condition  
907 and 20-53 neurons per well. **D** Percentage of isolectin B4-positive ( $IB4^+$ ) and -negative ( $IB4^-$ )  
908 mouse sensory neurons responding to 10  $\mu M$  of 5-oxoETE; n=3 independent experiments of 3  
909 wells per condition and 60 to 80 neurons per well. **E** Effects of 30 min incubation with PLC  
910 inhibitor (U73122; 10  $\mu M$ ) or overnight incubation with pertussis toxin (PTX; 250 ng/ml) on  
911 5-oxoETE-induced  $Ca^{2+}$  mobilization in mouse sensory neurons; n=5 independent experiments  
912 of 3 wells per condition and 60 to 80 neurons per well. Statistical analysis was performed using  
913 Kruskal-Wallis analysis of variance and subsequent Dunn's post hoc test. Data are mean  $\pm$   
914 SEM. \*  $p < 0.05$ , \*\*  $p < 0.01$ , \*\*\*  $p < 0.001$  significantly different from HBSS group.



Figure 5

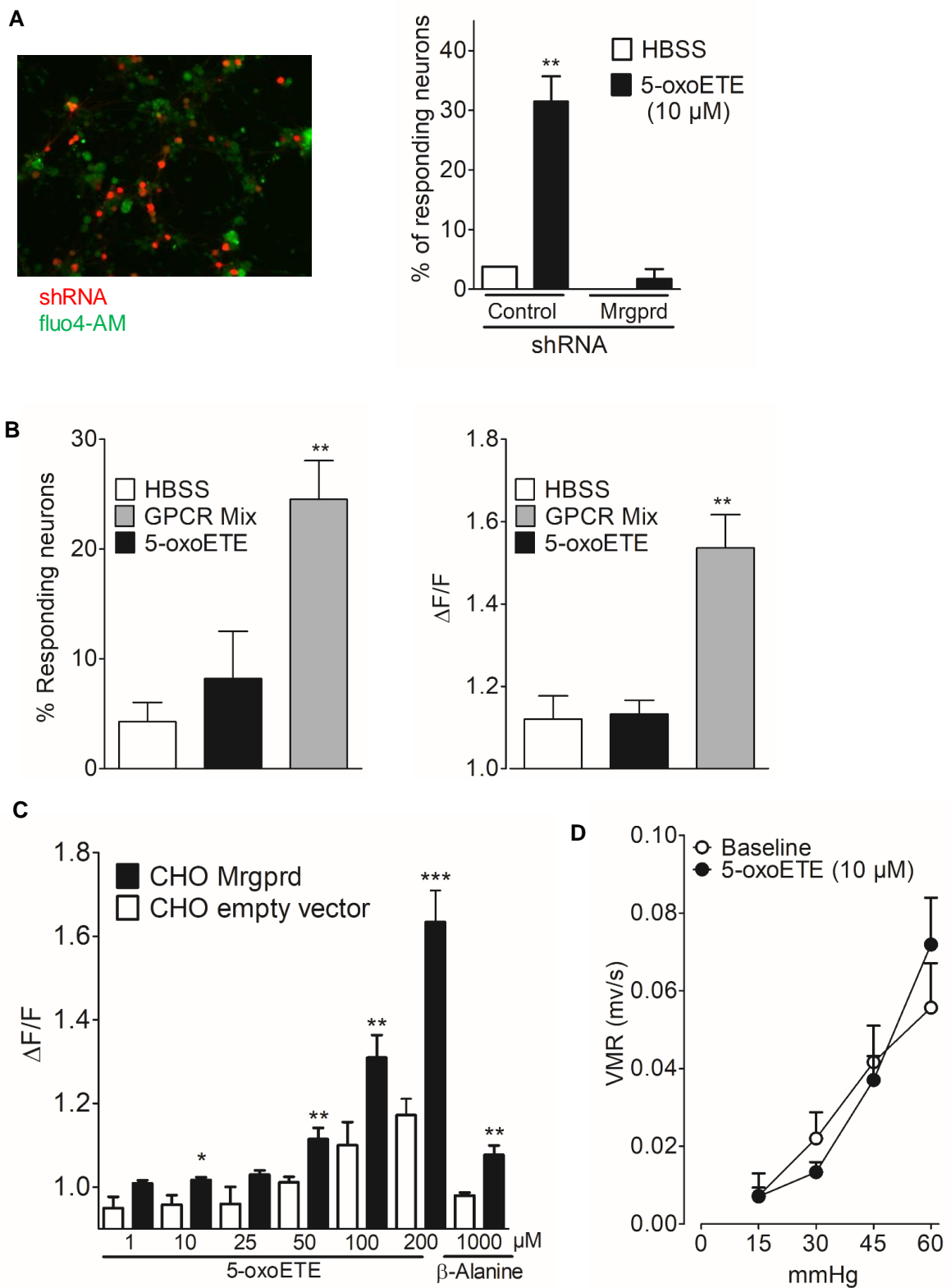


915

916 **Fig.5: Expression of *Mrgprd* in sensory neurons.** A Expression of *Mrgprd* (in red) and *trpv1*  
917 (in blue) mRNA transcripts by single-cell qRT-PCR (middle panel) of retrogradely labelled  
918 mouse colonic sensory neurons (left panel). Pie charts representation of the expression (dark

919 color) or not (light color) of *Mrgprd* and *Trpv1* mRNA in FB positive neurons (right panel),  
920 each segment represents a single colonic sensory neuron. **(B)** Representative images of GFP  
921 (green), CGRP- (red) immunoreactivity and FB labelling (blue) in a T13 DRG from  
922 *Mrgprd*<sup>EGFP</sup> mouse where FB was injected into the colon (scale bar = 50 μm). Expression of  
923 *Mrgprd* in whole human dorsal root ganglia **(C)** and in primary culture of human sensory  
924 neurons **(D)**; human whole DRG T11 **(C)**, scale bar = 10 μm) or primary culture of sensory  
925 neurons **(D)**, scale bar = 10 μm).  
926

Figure 6



927

928 **Fig.6: Mrgprd expression is required for the intracellular calcium mobilization and**

929 **hypersensitivity induced by 5-oxoETE. A** Left panel, representative picture of sensory

930 neurons transfected with shRNA (in red) containing the calcium probe Fluo4 (in green); right

931 panel, percentage of shRNA directed against *Mrgprd* or control positive sensory neurons  
932 responding to 10  $\mu$ M of 5-oxoETE; n=6 independent experiments of 3 wells per conditions and  
933 10 to 32 analyzed neurons per well. **B** Percentage of responding neurons (right panel) and  
934 amplitude of intracellular calcium mobilization ( $\Delta F/F$ ; left panel) in mouse sensory neurons  
935 from *Mrgprd* deficient mice exposed to vehicle (HBSS; white bar), 5-oxoETE (10  $\mu$ M, black  
936 bar) or to a mix of GPCR agonist (GPCR Mix: bradykinin, serotonin and histamine, 10  $\mu$ M  
937 each; gray bar); n=4 independent experiments of 3 wells per condition and 20-50 neurons per  
938 well. **C** Effects of 5-oxoETE (1–200  $\mu$ M) and  $\beta$ -Alanine (positive control), 1 mM) on the  
939 amplitude ( $\Delta F/F$ ) of calcium mobilization in HEK cells transiently expressing *Mrgprd* or vector  
940 control; n=8 independent experiments of 3 wells per condition. **D** Visceromotor response  
941 (VMR) in *Mrgprd* deficient mice to increasing pressures of colorectal distension before  
942 (baseline; white circle) and 30 min after intracolonic administration of 5-oxoETE (10  $\mu$ M; black  
943 circle); n=2 experiments of 7 mice. Data are mean  $\pm$  SEM. Statistical analysis was performed  
944 using Kruskal-Wallis analysis of variance and subsequent Dunn's post hoc test. \*\* p<0.01  
945 significantly different from control shRNA/HBSS group (**A**); \*\*p<0.01 significantly different  
946 from HBSS group (**B**); \* p<0.05; \*\*p<0.01; \*\*\* p<0.001 significantly different from the  
947 corresponding CHO empty vector group (**C**).

948